19

Variational Perturbation Theory

A powerful and yet mathematically simple method of resumming divergent perturbation expansions for critical exponents is provided by *variational perturbation theory*. This is a systematic extension of a variational approximation to path integrals, proposed some time ago by Feynman and Kleinert [1], to any desired order and accuracy [2]. The understanding of its convergence properties was greatly helped by pioneering mathematical work of Seznec and Zinn-Justin [3]. For an anharmonic oscillator, the expansions of energy eigenvalues converge uniformly and exponentially fast, like $e^{-\text{const}\times L^{1/3}}$ in the order L of the approximation. The uniformity of the convergence makes it possible to derive convergent strong-coupling expansions from divergent weak-coupling expansions. It turns out that the speed of convergence of the approach is governed by the finite convergence radius of the strong-coupling expansion: the constant in the above exponential is directly related to the convergence radius [4].

Since convergent strong-coupling expansions can be obtained so easily from divergent weak-coupling expansions, it is straightforward to develop a simple algorithm for finding uniformly convergent optimal inteations to functions for which both several weak-coupling and strong-coupling expansion coefficients are known [5].

19.1 From Weak- to Strong-Coupling Expansions

We shall apply this algorithm to the calculation of the renormalization constants of ϕ^4-theories for *all* coupling strengths, from which we can extract the limit of infinite bare coupling constant λ_B. As we shall see, this limit corresponds precisely to the fixed point g^* of the renormalized coupling g. The reason for this is that a perturbation expansion of the ϕ^4-theory in $4-\varepsilon$ dimensions produces series of the form

$$f_L(g_B) = \sum_{n=0}^{L} f_n g_B^n, \tag{19.1}$$

where $g_B = \lambda_B/\mu^\varepsilon$ is the dimensionless bare coupling constant. In a massive theory, the mass parameter μ can be chosen to be equal to the renormalized mass m. The approach to the critical point $m \to 0$ corresponds then to the limit $g_B \to \infty$, which is the same as the strong-coupling limit in the bare coupling constant λ_B. By performing this limit, we shall be able to reproduce the critical exponents obtained in the last chapter from the renormalization group equation.

19.2 Strong-Coupling Theory

Let us first explain in general how a divergent weak-coupling expansion of the type (19.1) may be turned into a strong-coupling expansion

$$f^M(g_B) = g_B^{p/q} \sum_{m=0}^{M} b_m (g_B^{-2/q})^m, \tag{19.2}$$

which has a finite convergence radius g_s. The leading power p/q of g_B is the parameter s in the previous resummation procedure in Eqs. (16.54), (16.61), and in Subsection 16.6.1.

Examples treated in the literature [5] are the anharmonic oscillator with parameters $p = 1/3,\ q = 3$ for the energy eigenvalues; and the Fröhlich polaron with $p = 1,\ q = 1$ for the ground-state energy, and $p = 4,\ q = 1$ for the mass. For the mass of the polaron, the summation gives quite different results from Feynman's, calling for further studies of this system.

The first step is to rewrite the weak-coupling expansion with the help of an auxiliary scale parameter κ [6]:

$$f_L(g_B) = \kappa^p \sum_{n=0}^{L} f_n \left(\frac{g_B}{\kappa^q}\right)^n, \tag{19.3}$$

where κ is eventually set equal to 1. We shall see below that the quotient p/q parametrizes the *leading power behavior* in g_B of the strong-coupling expansion, whereas $2/q$ characterizes the *approach* to the leading power behavior.

In the second step, we replace κ by the identical expression

$$\kappa \to \sqrt{K^2 + \kappa^2 - K^2} \tag{19.4}$$

containing a dummy scaling parameter K. The series (19.3) is then re-expanded in powers of g_B up to the order L, thereby treating $\kappa^2 - K^2$ as a quantity of order g_B. The result is most conveniently expressed in terms of dimensionless parameters $\hat{g}_B \equiv g_B/K^q$ and $\sigma(K) \equiv (1 - \hat{\kappa}^2)/\hat{g}_B$, where $\hat{\kappa} \equiv \kappa/K$ [suppressing g_B and κ in the arguments of $\sigma(K)$]. Then the replacement (19.4) becomes

$$\kappa \longrightarrow K(1 - \sigma\hat{g}_B)^{1/2}, \tag{19.5}$$

so that the re-expanded series reads explicitly

$$W_L(g_B, K) = K^p \sum_{n=0}^{L} \varepsilon_n(\sigma(K))\hat{g}_B^n, \tag{19.6}$$

with the coefficients:

$$\varepsilon_n(\sigma) = \sum_{j=0}^{n} f_j \begin{pmatrix} (p - qj)/2 \\ n - j \end{pmatrix} (-\sigma)^{n-j}. \tag{19.7}$$

For any fixed g_B and κ, we form the first and second derivatives of $W_L(g_B, K)$ with respect to K, calculate the K-values of the extrema and the turning points, and select the smallest of these as the optimal scaling parameter K_L. The function $W_L(g_B) \equiv W_L(g_B, K_L)$ constitutes the Lth variational approximation $f_L(g_B)$ to the function $f(g_B)$.

It is easy to take this approximation to the strong-coupling limit $g_B \to \infty$. For this we observe that (19.6) depends on its variables as follows:

$$W_L(g_B, K) = K^p w_L(\hat{g}_B, \hat{\kappa}^2). \tag{19.8}$$

For dimensional reasons, the optimal K_L increases for large g_B like $K_L \approx g_B^{1/q} c_L$, so that $\hat{g}_B$ becomes asymptotically constant, say $\hat{g}_B \to c_L^{-q}$ and $\sigma \to 1/\hat{g}_B \to c_L^q$, implying that they remain finite in the strong-coupling limit. The dimensionless $\hat{\kappa}^2$ tends to zero like $1/[c_L(g_B/\kappa^q)^{1/q}]^2$. Thus $W_L(g_B, K_L)$ behaves for large g_B like

$$W_L(g_B, K_L) \approx g_B^{p/q} c_L^p w_L(c_L^{-q}, 0). \tag{19.9}$$

In this limiting form, c_L plays the role of the variational parameter to be determined by the optimal extremum or turning point of $c_L^p w_L(c_L^{-q}, 0)$.

The full strong-coupling expansion is obtained by expanding $w_L(\hat{g}_B, \hat{\kappa}^2)$ in powers of $\hat{\kappa}^2 = (g_B/\kappa^q \hat{g}_B)^{-2/q}$ at $\hat{g}_B = c_L^{-q}$. The result is

$$W_L(g_B) = g_B^{p/q} \left[\bar{b}_0(\hat{g}_B) + \bar{b}_1(\hat{g}_B) \left(\frac{g_B}{\kappa^q} \right)^{-2/q} + \bar{b}_2(\hat{g}_B) \left(\frac{g_B}{\kappa^q} \right)^{-4/q} + \dots \right] \tag{19.10}$$

with

$$\bar{b}_n(\hat{g}_B) = \frac{1}{n!} w_L^{(n)}(\hat{g}_B, 0) \hat{g}_B^{(2n-p)/q}, \tag{19.11}$$

where $w_L^{(n)}(\hat{g}_B, \hat{\kappa}^2)$ is the nth derivative of $w_L(\hat{g}_B, \hat{\kappa}^2)$ with respect to $\hat{\kappa}^2$. Explicitly:

$$\frac{1}{n!} w_L^{(n)}(\hat{g}_B, 0) = \sum_{l=0}^{L} (-1)^{l+n} \sum_{j=0}^{l-n} f_j \begin{pmatrix} (p-qj)/2 \\ l-j \end{pmatrix} \begin{pmatrix} l-j \\ n \end{pmatrix} (-\hat{g}_B)^j. \tag{19.12}$$

The optimal expansion of the energy (19.10) is found by expanding

$$\hat{g}_B = c_L^{-q} \left[1 + \gamma_1 \left(\frac{g_B}{\kappa^q} \right)^{-2/q} + \gamma_2 \left(\frac{g_B}{\kappa^q} \right)^{-4/q} + \dots \right], \tag{19.13}$$

and finding the optimal extremum (or turning point) in the resulting polynomials of $\gamma_1, \gamma_2, \dots$. Setting the auxiliary scale parameter equal to unity, we obtain a strong-coupling expansion in powers of $g_B^{-2/q}$:

$$W_L(g_B) = g_B^{p/q} \left[b_0 + b_1 (g_B)^{-2/q} + b_2 (g_B)^{-4/q} + \dots \right], \tag{19.14}$$

which is of the desired type (19.2). In practice, the coefficients b_n are determined successively as follows. First we optimize $\bar{b}_0(\hat{g}_B)$ at $\hat{g}_B = c_L^{-q}$ and obtain $b_0 = \bar{b}_0(c_L^{-q})$. At the same value of $\hat{g}_B$ we calculate $b_1 = \bar{b}_1(c_L^{-q})$ and the coefficients $\bar{b}_i(c_L^{-q})$ $(i = 2, 3, \dots)$, and their derivatives $\bar{b}_i'(c_L^{-q})$, $\bar{b}_i''(c_L^{-q}) \dots$. From these we determine the remaining optimized coefficients b_i in the strong-coupling expansion (19.14) by combining $\bar{b}_i(c_L^{-q})$, as specified in Table 19.1 .

TABLE 19.1 Combinations of functions $\bar{b}_n(c_L^{-q})$ determining coefficients b_n of strong-coupling expansion (19.14). The arguments c_L^{-q} of $\bar{b}_n, \bar{b}_n', \bar{b}_n''$ are suppressed.

m	b_m	$-\gamma_{m-1}$
2	$\bar{b}_2 + \gamma_1 \bar{b}_1' + \frac{1}{2}\gamma_1^2 \bar{b}_0''$	$\bar{b}_1'/\bar{b}_0''$
3	$\bar{b}_3 + \gamma_2 \bar{b}_1' + \gamma_1 \bar{b}_2' + \gamma_1\gamma_2 \bar{b}_0'' + \frac{1}{2}\gamma_1^2 \bar{b}_1'' + \frac{1}{6}\gamma_1^3 \bar{b}_0^{(3)}$	$(\bar{b}_2' + \gamma_1 \bar{b}_1'' + \frac{1}{2}\gamma_1^2 \bar{b}_0^{(3)})/\bar{b}_0''$
4	$\bar{b}_4 + \gamma_3 \bar{b}_1' + \gamma_2 \bar{b}_2' + \gamma_1 \bar{b}_3' + (\frac{1}{2}\gamma_2^2 + \gamma_1\gamma_3)\bar{b}_0''$ $+\gamma_1\gamma_2 \bar{b}_1'' + \frac{1}{2}\gamma_1^2 \bar{b}_2'' + \frac{1}{2}\gamma_1^2\gamma_2 \bar{b}_0^{(3)} + \frac{1}{6}\gamma_1^3 \bar{b}_1^{(3)} + \frac{1}{24}\gamma_1^4 \bar{b}_0^{(4)}$	$(\bar{b}_3' + \gamma_2 \bar{b}_1'' + \gamma_1 \bar{b}_2'' + \gamma_1\gamma_2 \bar{b}_0^{(3)}$ $+\frac{1}{2}\gamma_1^2 \bar{b}_1^{(3)} + \frac{1}{6}\gamma_1^3 \bar{b}_0^{(4)})/\bar{b}_0''$

This procedure will be applied to renormalization group functions in Sections 19.5 and 20.1. There we shall be dealing only with functions $f(g_B)$ which go to a constant f_L^* in the strong-coupling limit. Thus we have $p = 0$, and the critical exponents follow from the first term in the expansions (19.14). It is given by (19.11) for $n = 0$, which we shall write as

$$f_L^* = \operatorname*{opt}_{\hat{g}_B} \left[\sum_{l=0}^{L} f_l \hat{g}_B^l \sum_{k=0}^{L-l} \binom{-ql/2}{k} (-1)^k \right], \tag{19.15}$$

where the expression in square brackets has to be optimized in the variational parameter $\hat{g}_B$. Mnemonically, a better way to express this formula is

$$f_L^* = \operatorname*{opt}_{\hat{g}_B} \left[\sum_{l=0}^{L} f_l \hat{g}_B^l \, [1-1]_{L-l}^{-ql/2} \right], \tag{19.16}$$

where the symbol $[1-x]_{L-l}^{-ql/2}$ denotes the binomial expansion of $(1-x)^{-ql/2}$ up to the power $L-l$ in the second argument x:

$$[1-x]_{L-l}^{-ql/2} \equiv \sum_{k=0}^{L-l} \binom{-ql/2}{k} (-x)^k. \tag{19.17}$$

19.3 Convergence

The number of weak-coupling coefficients calculated so far for ϕ^4-theories in $4-\varepsilon$ dimensions is limited to $L = 5$ (see Chapter 17). Thus it will be important to know the specific way in which the approximations $W_L(g_B)$ approach the final result $W_\infty(g_B)$. We shall derive this behavior in general [6, 7] for any strong-coupling parameters p and q. Let us remove the factor κ^p from the function $f(g_B)$, defining the reduced quantity $\tilde{f}(\tilde{g}_B) = f(g_B)/\kappa^p$ as a function of the reduced coupling constant $\tilde{g}_B \equiv g_B/\kappa^q$. We further assume the strong-coupling growth $g_B^{p/q}$ of the function $f(g_B)$ to be less than linear, so that $\tilde{f}(\tilde{g}_B)$ satisfies a once-subtracted dispersion relation (compare the discussion in Section 16.1):

$$\tilde{f}(\tilde{g}_B) = f_0 + \frac{\tilde{g}_B}{2\pi i} \int_0^{-\infty} \frac{d\tilde{g}_B'}{\tilde{g}_B'} \frac{\operatorname{disc} \tilde{f}(\tilde{g}_B')}{\tilde{g}_B' - \tilde{g}_B}, \tag{19.18}$$

where $\operatorname{disc} \tilde{f}(\tilde{g}_B)$ is the discontinuity across the left-hand cut in the complex g_B-plane:

$$\operatorname{disc} \tilde{f}(\tilde{g}_B) = \tilde{f}(\tilde{g}_B + i\eta) - \tilde{f}(\tilde{g}_B - i\eta) = 2\,i\,\operatorname{Im} \tilde{f}(\tilde{g}_B + i\eta) \quad \text{for } \tilde{g}_B < 0, \tag{19.19}$$

with η being an infinitesimal positive number. An expansion of the integrand in powers of $\tilde{g}_B$ up to $\tilde{g}_B^L$ reproduces of course the initial perturbation series (19.3), where the expansion coefficients are moment integrals over the discontinuity:

$$a_k = \frac{1}{2\pi i} \int_{-\infty}^{0} \frac{d\tilde{g}_B}{\tilde{g}_B^{k+1}} \operatorname{disc} \tilde{f}(\tilde{g}_B). \tag{19.20}$$

The dispersion relation (19.18) can also be used to derive moment integrals for the re-expansion coefficient $\varepsilon_l(\sigma)$ in (19.6) and (19.7). For the dimensionless coupling constant $\tilde{g}_B$, the replacement (19.5) becomes

$$\tilde{g}_B \longrightarrow \tilde{G}_B(\hat{g}_B) \equiv \frac{\hat{g}_B}{(1-\sigma \hat{g}_B)^{q/2}}. \tag{19.21}$$

Because of the prefactor κ^p in (19.3), the replacement (19.4) also produces a prefactor $K^p/\kappa^p = (1-\sigma\hat{g}_B)^{p/2}$ to the function $f(g_B)$. For the reduced function $\hat{f}(\hat{g}_B) \equiv f(g_B)/K^p$, which depends only on the reduced coupling constant $\hat{g}_B$, we thus obtain a dispersion relation

$$\hat{f}(\hat{g}_B) = (1-\sigma\hat{g}_B)^{p/2}\left[f_0 + \frac{\tilde{G}_B(\hat{g}_B)}{2\pi i}\int_{-\infty}^{0}\frac{d\tilde{g}'_B}{\tilde{g}'_B}\frac{\mathrm{disc}\,\tilde{f}(\tilde{g}'_B)}{\tilde{g}'_B - \tilde{G}_B(\hat{g}_B)}\right]. \tag{19.22}$$

This function satisfies a dispersion relation in the complex $\hat{g}_B$-plane. If C denotes the image of the left-hand cut in the original dispersion relation (19.18) as it arises from the mapping (19.21), and if $\mathrm{disc}_C f(\hat{g}_B)$ denotes the discontinuity across this cut, the dispersion relation reads

$$\hat{f}(\hat{g}_B) = f_0 + \frac{\hat{g}_B}{2\pi i}\int_C \frac{d\hat{g}'_B}{\hat{g}'_B}\frac{\mathrm{disc}_C\hat{f}(\hat{g}'_B)}{\hat{g}'_B - \hat{g}_B}. \tag{19.23}$$

An expansion of the integrand in powers of $\hat{g}_B$ yields moment integrals for the desired re-expansion coefficients $\varepsilon_k(\sigma)$:

$$\varepsilon_k(\sigma) = \frac{1}{2\pi i}\int_C \frac{d\hat{g}_B}{\hat{g}_B^{k+1}}\mathrm{disc}_C\hat{f}(\hat{g}_B). \tag{19.24}$$

The discontinuity in these integrals can be derived from the dispersion relation (19.22). The function $\tilde{G}_B(\hat{g}_B)$ in (19.21) carries the left-hand cut in the complex $\tilde{g}_B$-plane over into several cuts in the $\hat{g}_B$-plane. In Fig. 19.1 we show the image cuts for $q = 3$, where the critical exponent

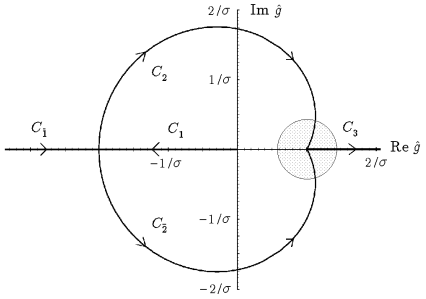

FIGURE 19.1 Image of left-hand cut in complex $\hat{g}_B$-plane for $q = 3$ -mapping (19.21).

of the approach to scaling is $\omega = 2/3$, as in the quantum-mechanical anharmonic oscillator. The cuts run along the contours $C_1,\ C_{\bar{1}},\ C_2\ , C_{\bar{2}},\ C_3$, the last being caused by the powers $q/2$ and $p/2$ of $1-\sigma\hat{g}_B$ in the mapping (19.21) and the prefactor in (19.22), respectively. Let $\tilde{D}(\tilde{g}_B)$ abbreviate the reduced discontinuity (19.19):

$$\tilde{D}(\tilde{g}_B) \equiv \mathrm{disc}\tilde{f}(\tilde{g}_B) = 2i\mathrm{Im}\,\tilde{f}(\tilde{g}_B + i\eta), \qquad \tilde{g}_B \le 0. \tag{19.25}$$

Then the discontinuities across the various cuts are

$$\underset{C_{1,\bar{1},2,\bar{2}}}{\mathrm{disc}}\ \hat{f}(\hat{g}_B) \;=\; (1-\sigma\hat{g}_B)^{p/2}\tilde{D}(\hat{g}_B(1-\sigma\hat{g}_B)^{-q/2}), \tag{19.26}$$

$$\underset{C_3}{\mathrm{disc}}\ \hat{f}(\hat{g}_B) \;=\; -2i(\sigma\hat{g}_B - 1)^{p/2}\times\left[f_0 + \int_0^\infty \frac{d\tilde{g}'_B}{2\pi}\frac{\hat{g}_B(\sigma\hat{g}_B-1)^{-q/2}}{\tilde{g}'^2_B + \hat{g}_B^2(\sigma\hat{g}_B-1)^{-q}}\tilde{D}(-\tilde{g}'_B)\right]. \tag{19.27}$$

For small negative $\tilde{g}_B$, the discontinuity is given by a standard semiclassical approximation with the typical form

$$\tilde{D}(\tilde{g}_B) \approx i\ \mathrm{const}\times\tilde{g}_B^b\, e^{a/\tilde{g}_B}. \tag{19.28}$$

The exponential plays the role of a Boltzmann factor for the activation of a classical solution to the field equations, whereas the prefactor accounts for the entropy of the field fluctuations around this solution.

Let us denote by $\varepsilon_k(C_i)$ the contributions of the different cuts to the integral (19.24). After inserting (19.28) into (19.26), we obtain from the cut along C_1 the semiclassical approximation

$$\varepsilon_k(C_1) \approx \text{const} \times \int_{C_1} \frac{d\hat{g}_B}{2\pi} \frac{1}{\hat{g}_B^{k+1}} (1-\sigma\hat{g}_B)^{p/2-bq/2} \hat{g}_B^b \, e^{a(1-\sigma\hat{g}_B)^{q/2}/\hat{g}_B}. \tag{19.29}$$

For the kth term of the series $S_k \equiv \varepsilon_k \hat{g}_B^k$, this yields the large-$k$ estimate

$$S_k \propto \left[\int_{C_\gamma} \frac{d\gamma}{2\pi} e^{h_k(\gamma)} \right] \gamma^k, \tag{19.30}$$

where $\gamma \equiv \sigma\hat{g}_B$, and $h_k(\gamma)$ is the function

$$h_k(\gamma) \approx -k\log(-\gamma) + \frac{a\sigma}{\gamma}(1-\gamma)^{q/2} + (b-1)\log(-\gamma) + \dots \ . \tag{19.31}$$

For large k, the saddle point approximation yields via the extremum at $\gamma \underset{k\to\infty}{\longrightarrow} \gamma_k = -a\sigma/k$:

$$h_k \underset{k\to\infty}{\longrightarrow} k\log(k/ea\sigma) - aq\sigma/2 + (b-1)\log\frac{a\sigma}{k} + \dots \ . \tag{19.32}$$

The constant $-aq\sigma/2$ in this limiting expression arises when expanding the second term of Eq. (19.31) into a Taylor series, $(a\sigma/\gamma)(1-\gamma)^{q/2} = a\sigma/\gamma_k - aq\sigma/2 + \dots$. Only the first two terms in (19.32) contribute to the large-k limit. Thus, to leading order in k, the kth term of the re-expanded series becomes

$$S_k \propto e^{-aq\sigma/2} \left(\frac{-k}{e}\right)^k \hat{g}^k. \tag{19.33}$$

The corresponding re-expansion coefficients

$$\varepsilon_k \propto e^{-aq\sigma/2} f_k \tag{19.34}$$

have the remarkable property of growing in precisely the same manner with k as the initial expansion coefficients h_k, except for an overall suppression factor $e^{-aq\sigma/2}$.

To estimate the convergence of the variational perturbation expansion (19.6), we note that $\sigma\hat{g} = 1-\hat{\kappa}^2$ is smaller than unity for large K, so that the powers $(\sigma\hat{g})^k$ by themselves would yield a convergent series. An optimal re-expansion of the reduced function $\hat{f}(\hat{g}_B)$ can be achieved by choosing, for a given large maximal order L of the expansion, a parameter σ proportional to L:

$$\sigma \approx \sigma_L \equiv cL. \tag{19.35}$$

Inserting this into (19.31), we obtain for large $k = L$

$$h_L(\gamma) \approx L\left[-\log(-\gamma) + \frac{ac}{\gamma}(1-\gamma)^{q/2}\right]. \tag{19.36}$$

The extremum of this function lies at a γ-value satisfying the equation

$$1 + \frac{ac}{\gamma}(1-\gamma)^{q/2-1}\left[1 + \left(\frac{q}{2}-1\right)\gamma\right] = 0. \tag{19.37}$$

The constant c may be chosen in such a way that the large exponent proportional to L in the exponential function $e^{h_L(\gamma)}$ arising from the first term in (19.36) is canceled by an equally large contribution from the second term, i.e., we require at the extremum

$$h_L(\gamma) = 0. \tag{19.38}$$

The two equations (19.37) and (19.38) are solved by certain constant values of $\gamma < 0$ and c. In contrast to the extremal γ of Eq. (19.31) which dominates the large-k limit, the extremal γ in the present limit, in which k is also large but of the same size as L, remains finite (the previous estimate held for $k \gg L$). Accordingly, the second term $(ac/\gamma)(1-\gamma)^{q/2}$ in $h_L(\gamma)$ contributes in full, not merely via the first two Taylor expansion terms of $(1-\gamma)^{q/2}$ as it did in (19.32).

Since $h_L(\gamma)$ vanishes at the extremum, the Lth term in the re-expansion has the order of magnitude

$$S_L(C_1) \propto (\sigma_L \hat{g}_B)^L = \left(1 - \frac{1}{K_L^2}\right)^L. \tag{19.39}$$

According to (19.35), the scale parameter K_L grows for large L like

$$K_L \sim \sigma_L^{1/q} g_B^{1/q} \sim (cLg_B)^{1/q}. \tag{19.40}$$

As a consequence, the last term of the series decreases for large L like

$$S_L(C_1) \propto \left[1 - \frac{1}{(\sigma_L g_B)^{2/q}}\right]^L \approx e^{-L/(\sigma_N g_B)^{2/q}} \approx e^{-L^{1-2/q}/(cg_B)^{2/q}}. \tag{19.41}$$

This estimate does not yet explain the exponentially fast convergence of the variational perturbation expansion in the strong-coupling limit [8]. For the contribution of the cut C_1 to S_L, the derivation of such a behavior requires including the approach of σ_L to the large-L behavior (19.35), which has the same general form as the strong-coupling expansion (19.10),

$$\sigma_L \sim cL\left(1 + \frac{c'}{L^{2/q}} + \ldots\right), \tag{19.42}$$

as it turns out with positive c'. By inserting this σ_L into $h_L(\gamma)$ of (19.36), we find an extra exponential factor which dominates the large-L behavior at infinite coupling $\hat{g}_B$:

$$e^{\Delta h_L} \approx \exp\left[-L\log(-\gamma)\frac{c'}{L^{2/q}}\right] \approx e^{-c''L^{1-2/q}}. \tag{19.43}$$

What about the contributions of the other cuts? For $C_{\bar{1}}$, the integral in (19.24) runs from $\hat{g} = -2/\sigma$ to $-\infty$ and decrease like $(-2/\sigma)^{-k}$. The associated last term $S_L(C_{\bar{1}})$ is of the negligible order $e^{-L\log L}$. For the cuts $C_{2,\bar{2},3}$, the integral (19.24) starts at $\hat{g} = 1/\sigma$ and has therefore the leading behavior

$$\varepsilon_k(C_{2,\bar{2},3}) \sim \sigma^k, \tag{19.44}$$

yielding at first a contribution to the Lth term in the re-expansion of the order of

$$S_L(C_{2,\bar{2},3}) \sim (\sigma\hat{g})^L, \tag{19.45}$$

which decreases merely like (19.41) and does not explain the empirically observed convergence in the strong-coupling limit. The important additional information [9] is that the cuts in Fig. 19.1 do not really reach the point $\sigma\hat{g} = 1$. There exists a small circle of radius $\Delta\hat{g} > 0$ in which $\hat{f}(\hat{g})$

has no singularities at all. This is a consequence of the fact, unused up to this point, that the strong-coupling expansion (19.10) converges for $g_B > g_s$. For the reduced function $\hat{f}(\hat{g}_B)$, this expansion reads

$$\hat{f}(\hat{g}) = (\hat{g}_B)^{p/q} \left\{ b_0 + b_1 \left[\frac{\hat{g}_B}{(1-\sigma\hat{g}_B)^{q/2}} \right]^{-2/q} + b_2 \left[\frac{\hat{g}_B}{(1-\sigma\hat{g}_B)^{q/2}} \right]^{-4/q} + \dots \right\}. \tag{19.46}$$

The convergence of (19.10) for $g_B > g_s$ implies that (19.46) converges for all $\sigma\hat{g}_B$ in a neighborhood of the point $\sigma\hat{g}_B = 1$ with a radius

$$\Delta(\sigma\hat{g}_B) = \left| \frac{\hat{g}_B}{\tilde{g}_s} \right|^{2/q}, \tag{19.47}$$

where $\tilde{g}_s \equiv g_s/\kappa^q$. For large L, the denominator K^q in $\hat{g}_B$ on the right-hand side makes $\Delta(\sigma\hat{g}_B)$ go to zero like

$$\Delta(\sigma\hat{g}_B) \approx \frac{1}{(L|\tilde{g}_s|c)^{2/q}}. \tag{19.48}$$

Thus the integration contours of the moment integrals (19.24) for the contributions $\varepsilon_k(C_i)$ of the other cuts do not begin at the point $\sigma\hat{g} = 1$, but a little distance $\Delta(\sigma\hat{g})$ away from it. If $q < 4$, i.e., if $\omega > 1/2$, the intersection points of the small circle with the cuts C_2 and $C_{\bar{2}}$ have a real part larger than unity. This produces a suppression factor to the previous result (19.44) of the integral (19.24):

$$(\sigma\hat{g}_B)^{-L} \sim [1 + \Delta(\sigma\hat{g}_B)]^{-L}, \tag{19.49}$$

bringing the last term of the series S_L to

$$S_L(C_{2,\bar{2},3}) \sim (\sigma\hat{g}_B)^L \frac{1}{[1+\Delta(\sigma\hat{g}_B)]^L} \tag{19.50}$$

instead of (19.45). Inserting (19.48), we find that this goes to zero with the same characteristic behavior (19.43) as the contribution from the cut C_1:

$$S_L(C_{2,\bar{2},3}) \approx e^{-c''' L^{1-\omega}}, \qquad c''' > 0. \tag{19.51}$$

Such a behavior therefore characterizes the convergence for $L \to \infty$, which will be needed in Sections 19.5 and 20.1 to extrapolate finite-L results to $L \to \infty$.

19.4 Strong-Coupling Limit and Critical Exponents

In the examples treated in the original Ref. [6], the strong-coupling parameters p and q were known. In the present field system, only p is known to be zero if we assume the system to have experimentally observed scaling properties. Then there exists an infrared-stable fixed point g^*, and the strong-coupling expansion for the expansion of g in powers of g_B will have a large-g_B behavior of the form [10]

$$g(g_B) = g^* - \frac{\text{const}}{g_B^{\omega/\varepsilon}} + \dots . \tag{19.52}$$

The assumption of a strong-coupling scaling of this form is equivalent to the assumption that the β-function has a zero g^*. Rewriting the β-function as $-\varepsilon dg/d\log g_B$ and integration with Eq. (10.103) results in (19.52).

In the general framework of Section 19.2, we have to resum the series

$$g_L = \sum_{n=1}^{L} f_n g_B^n \tag{19.53}$$

with the strong-coupling parameters $p = 0$ and $q = 2\varepsilon/\omega$ [compare expansion (19.10)].

Both p and q can be determined to any desired accuracy from the power series which we want to resum. Indeed, the ratios p/q and $2/q$ are obtainable from the strong-coupling limits of the following infinite set of logarithmic derivatives of $W_L(g_B)$:

$$\frac{p}{q} = F_1(\infty), \qquad F_1(g_B) \equiv \frac{d\log W_L(g_B)}{d\log g_B} = g_B \frac{W_L'(g_B)}{W_L(g_B)}, \tag{19.54}$$

$$-\frac{2}{q} - 1 = F_2(\infty), \qquad F_2(g_B) \equiv \frac{d\log F_1'(g_B)}{d\log g_B} = g_B \frac{F_1''(g_B)}{F_1'(g_B)}. \tag{19.55}$$

Under the assumption that the strong-coupling expansion contains only powers of $g_B^{-\omega}$, there is an infinite set of further equations

$$-\frac{2}{q} - 1 = F_3(\infty), \qquad F_3(g_B) \equiv \frac{d\log F_2'(g_B)}{d\log g_B} = g_B \frac{F_2''(g_B)}{F_2'(g_B)}, \tag{19.56}$$

$$-\frac{2}{q} - 1 = F_4(\infty), \qquad F_4(g_B) \equiv \frac{d\log F_3'(g_B)}{d\log g_B} = g_B \frac{F_3''(g_B)}{F_3'(g_B)}, \tag{19.57}$$

$$\vdots \quad .$$

For the anharmonic oscillator, these equations are all satisfied. In the field theoretic perturbation expansions the possible presence of *confluent singularities* [11] containing powers of $g_B^{-\omega'}$, $g_B^{-\omega''}$ with exponents $\omega'' > \omega' > \omega$ makes the higher equations unreliable.

If the parameter p happens to be zero, which is the case in the application to be considered, there is a further formula for the parameter q:

$$-\frac{2}{q} - 1 = G_1(\infty), \qquad G_1(g_B) \equiv \frac{d\log W_L'(g_B)}{d\log g_B} = g_B \frac{W_L''(g_B)}{W_L'(g_B)}. \tag{19.58}$$

and in the absence of confluent singularities a further sequence of equations

$$-\frac{2}{q} - 1 = G_2(\infty), \qquad G_2(g_B) \equiv \frac{d\log G_1'(g_B)}{d\log g_B} = g_B \frac{G_1''(g_B)}{G_1'(g_B)}, \tag{19.59}$$

$$-\frac{2}{q} - 1 = G_3(\infty), \qquad G_3(g_B) \equiv \frac{d\log G_2'(g_B)}{d\log g_B} = g_B \frac{G_2''(g_B)}{G_2'(g_B)}, \tag{19.60}$$

$$\vdots \quad .$$

Formulas (19.54) and (19.58) will be crucial to the development in Sections 19.5 and 20.1. They enable us to calculate the critical exponent ω of the approach to scalingfrom the power series expansion (19.53).

When applied to the expansion of $g(g_B)$, the logarithmic derivative (19.54) can be written as

$$\frac{p}{q} = s = g_B \frac{g'(g_B)}{g(g_B)}. \tag{19.61}$$

The function on the right-hand side is, up to a factor $-\varepsilon g(g_B)$, equal to the β-function (10.30) of the renormalization group analysis:

$$\beta(g_B) = -\varepsilon g_B g'(g_B). \tag{19.62}$$

This follows directly from the defining equation (10.30). Thus Eq. (19.61) can be rewritten as

$$\frac{p}{q} = s = -\frac{\beta(g_B)}{\varepsilon g(g_B)}, \tag{19.63}$$

and the property $s = 0$ is equivalent to the vanishing of the β-function in the ordinary renormalization group analysis.

The critical exponent ω will be calculated by requiring the resummed power series expansion for (19.63) to vanish in the strong-coupling limit, thus ensuring a constant limit $g \to g^*$:

$$0 = g_B \frac{g'(g_B)}{g(g_B)}\bigg|_{g_B=\infty}. \tag{19.64}$$

Alternatively we may also use Eq. (19.58) to determine

$$\frac{\omega}{\varepsilon} = -1 - g_B \frac{g''(g_B)}{g'(g_B)}\bigg|_{g_B=\infty}. \tag{19.65}$$

It is easy to verify that this equation is completely equivalent to Eq. (10.104), where ω is defined as the slope of the β-function at $g = g^*$. Indeed, differentiating the Eq. (19.62) for the β-function with respect to g, the chain rule leads directly to (19.65). Equation (19.64) will be used to determine $q = 2\varepsilon/\omega$ directly to make the strong-coupling limit vanish. For comparison, the other equation (19.65) will sometimes be solved as well. This is done recursively, determining the left-hand side using some initial trial ω in the strong-coupling limit of the right-hand side, and repeating the procedure with the new ω until it converges. This procedure will be referred to as the self-consistent determination of ω.

The same exponent ω can be found from the series expansion of any function $f(g)$ of the renormalized coupling constant g in powers of the bare coupling constant g_B, which all behave for large g_B, due to (19.52), like

$$f(g) = f(g^*) + f'(g^*) \times \frac{\text{const}}{g_B^{\omega/\varepsilon}} + \dots\ . \tag{19.66}$$

From the definitions (10.20), (10.22), (10.23), (10.94), and (10.95) of the renormalization group functions, we deduce the alternative derivative equations for the critical exponents which are useful for the upcoming strong-coupling calculations:

$$\eta_m(g_B) = -\varepsilon \frac{d}{d\log g_B} \log \frac{m^2}{m_B^2}, \qquad \eta(g_B) = \varepsilon \frac{d}{d\log g_B} \log \frac{\phi^2}{\phi_B^2}. \tag{19.67}$$

If we set $\mu = m$, we find that $g_B = \lambda_B \mu^{-\varepsilon}$ goes to infinity like const $\times\, m^{-\varepsilon}$ for $m \to 0$. Thus the strong-coupling limit is approached for $m \to 0$, implying the power behavior

$$\frac{m^2}{m_B^2} \propto g_B^{-\eta_m/\varepsilon} \propto m^{\eta_m}, \qquad \frac{\phi^2}{\phi_B^2} \propto g_B^{\eta/\varepsilon} \propto m^{-\eta}, \tag{19.68}$$

where η_m and η are the $g\beta \to \infty$ -limits of $\eta_m(g_B)$ and $\eta(g_B)$, the first determining the critical exponent ν via $\nu = 1/(2-\eta_m)$.

When approaching a second-order phase transition, the bare square mass m_B^2 vanishes like $\tau \equiv T/T_c - 1$. The renormalized mass m^2 will vanish with a different power of τ. This power is obtained from the first equation in (19.68), which shows that $m \propto \tau^\nu$. Experiments observe that the coherence length of fluctuations $\xi = 1/m$ increases near T_c like $\tau^{-\nu}$. Similarly we see from the second equation in (19.68) that the scaling dimension $D/2-1$ of the bare field ϕ_B for $T \to T_c$ is changed, in the strong-coupling limit $g_B \to \infty$, to $D/2 - 1 + \eta/2$, the number η being the so-called anomalous dimension of the field. This implies a change in the large-distance behavior of the correlation functions $\langle \phi(\mathbf{x})\phi(\mathbf{0})\rangle$ at T_c from the free-field behavior r^{-D+2} to $r^{-D+2-\eta}$. The magnetic susceptibility is determined by the integrated correlation function $\langle \phi_B(\mathbf{x})\phi_B(\mathbf{0})\rangle$. At zero coupling constant g_B, this is proportional to $1/m_B^2 \propto \tau^{-1}$, which is changed by fluctuations to $m^{-2}\phi_B^2/\phi^2$. This has a temperature behavior $m^{-(2-\eta)} = \tau^{-\nu(2-\eta)} \equiv \tau^{-\gamma}$, which defines the critical exponent $\gamma = \nu(2-\eta)$ observable in magnetic experiments.

19.5 Explicit Low-Order Calculations

If the expansions are known to orders $L = 2$, 3, or 4, we can give analytic expressions for the strong-coupling limits (19.16).

19.5.1 General Formulas

Setting $\rho \equiv 1 + q/2 = 1 + \varepsilon/\omega$, we find for $L = 2$

$$f_2^* = \operatorname*{opt}_{\hat{g}_B} \left[f_0 + f_1 \rho \hat{g}_B + f_2 \hat{g}_B^2 \right] = f_0 - \frac{1}{4}\frac{f_1^2}{f_2}\rho^2. \tag{19.69}$$

For $L = 3$, we obtain from the extrema

$$\begin{aligned} f_3^* &= \operatorname*{opt}_{\hat{g}_B} \left[f_0 + \tfrac{1}{2} f_1 \rho(\rho+1)\hat{g}_B + f_2(2\rho-1)\hat{g}_B^2 + f_3 \hat{g}_B^3 \right] \\ &= f_0 - \frac{1}{3}\frac{\bar{f}_1 \bar{f}_2}{f_3}\left(1 - \frac{2}{3}r\right) + \frac{2}{27}\frac{\bar{f}_2^3}{f_3^2}(1-r), \end{aligned} \tag{19.70}$$

where $r \equiv \sqrt{1 - 3\bar{f}_1 f_3/\bar{f}_2^2}$ and $\bar{f}_1 \equiv \frac{1}{2} f_1 \rho(\rho+1)$ and $\bar{f}_2 \equiv f_2(2\rho-1)$. The positive square root must be taken to connect g_3^* smoothly to g_2^* in the limit of a vanishing coefficient of g_B^3. If the square root is imaginary, the optimum is given by the unique turning point, leading once more to (19.70) but with $r = 0$:

$$f_3^* = f_0 - \frac{1}{3}\frac{\bar{f}_1 \bar{f}_2}{f_3} + \frac{2}{27}\frac{\bar{f}_2^3}{f_3^2}. \tag{19.71}$$

The parameter $\rho = 1 + \varepsilon/\omega$ can be determined from the expansion coefficients of a function $F(g_B)$ as follows. Assuming $F(g_B)$ to be constant F^* in the strong-coupling limit, the logarithmic derivative $f(g_B) \equiv g_B F'(g_B)/F(g_B)$ must vanish at $g_B = \infty$ [see (19.64)].

If $F(g_B)$ starts out as $F_0 + F_1 g_B + \dots$ or $F_1 g_B + F_2 g_B^2 + \dots$, the logarithmic derivative is

$$f(g_B) = F_1' g_B + (2F_2' - F_1'^2) g_B^2 + (F_1'^3 - 3F_1'F_2' + 3F_3') g_B^3 + \dots , \tag{19.72}$$

where $F_i' = F_i/F_0$, or

$$f(g_B) = 1 + \hat{F}_2 g_B + (2\hat{F}_3 - \hat{F}_2^2) g_B^2 + (\hat{F}_2^3 - 3\hat{F}_2\hat{F}_3 + 3\hat{F}_4) g_B^3 + \dots , \tag{19.73}$$

where $\hat{F}_i = F_i/F_1$. The expansion coefficients on the right-hand sides are then inserted into (19.69) or (19.70), and the left-hand sides have to vanish to ensure that $F(g_B) \to F^*$.

If the approach $F(g_B) \to F^*$ is of the type (19.66), the function

$$h(g_B) \equiv g_B \frac{F''(g_B)}{F'(g_B)} = 2\hat{F}_2 g_B + (-4\hat{F}_2^2 + 6\hat{F}_3) g_B^2 + (8\hat{F}_2^3 - 18\hat{F}_2\hat{F}_3 + 12\hat{F}_4) g_B^3 + \dots \quad (19.74)$$

must have the strong-coupling limit [recall (19.65)]

$$h(g_B) \to h^* = -\frac{\omega}{\varepsilon} - 1. \quad (19.75)$$

This is true for both expansions $F_0 + F_1 g_B + \dots$ and $F_1 g_B + F_2 g_B^2 + \dots$.

19.5.2 Perturbation Series

The above formulas are now applied to the power series expansions of O(N)-symmetric ϕ^4-theories in $D = 4 - \varepsilon$ dimensions. Their renormalized coupling constant is related to the unrenormalized ones by Eq. (15.18), which we shall use at first only up to order $L = 3$:

$$\bar{g} = \bar{g}_B - \frac{(N+8)}{3\varepsilon}\bar{g}_B^2 + \left[\frac{(N+8)^2}{9\varepsilon^2} + \frac{(3N+14)}{6\varepsilon}\right]\bar{g}_B^3 + \dots . \quad (19.76)$$

Inserting this into the expansions (15.15) and (15.11), we obtain for the mass and field ratios

$$\frac{m^2}{m_B^2} = 1 - \frac{N+2}{3}\frac{\bar{g}_B}{\varepsilon} + \frac{(N+2)}{9}\left[\frac{N+5}{\varepsilon^2} + \frac{5}{4\varepsilon}\right]\bar{g}_B^2 + \dots , \quad (19.77)$$

$$\frac{\phi^2}{\phi_B^2} = 1 + \frac{N+2}{36}\frac{\bar{g}_B^2}{\varepsilon} + \dots . \quad (19.78)$$

Remember that the dimensionless bare coupling constant $\bar{g}_B$ contains the arbitrary mass scale μ given by

$$\bar{g}_B = \frac{g_B}{(4\pi)^2} = \frac{\lambda_B}{\mu^\varepsilon (4\pi)^2}.$$

The arbitrary mass scale μ will now be set equal to the physical mass m, as discussed at the beginning of this chapter and before Eq. (19.68), considering all quantities as functions of $\bar{g}_B$. In order to describe second-order phase transitions, we let m_B^2 go to zero proportionally to $\tau = T/T_c - 1$ as the temperature T approaches the critical temperature T_c. Then m^2 will also go to zero, and thus $\bar{g}_B$ to infinity.

We use the vanishing of (19.73) at infinite bare coupling $\bar{g}_B$, or Eq. (19.75) with (19.74), to determine the critical exponent of approach to scaling ω. For the other critical exponents we find from formulas (19.67), (19.77), and (19.78) the expansions

$$\eta_m(\bar{g}_B) = \frac{N+2}{3}\bar{g}_B - \frac{N+2}{18}\left(5 + 2\frac{N+8}{\varepsilon}\right)\bar{g}_B^2, \quad (19.79)$$

$$\eta(\bar{g}_B) = \frac{N+2}{18}\bar{g}_B^2. \quad (19.80)$$

The scaling relation $\gamma = \nu(2-\eta)$ with $\nu = 1/(2-\eta_m)$ and the expansions (19.79), (19.80) yield for the critical exponent $\gamma(g_B)$ of the susceptibility defined in Eq. (10.160) the perturbation expansion up to second order in g_B:

$$\gamma(\bar{g}_B) = 1 + \frac{N+2}{6}\bar{g}_B + \frac{N+2}{36}\left(N - 4 - 2\frac{N+8}{\varepsilon}\right)\bar{g}_B^2. \quad (19.81)$$

We shall evaluate this rather than the series (19.80) for $\eta(\bar{g}_B)$, since $\gamma(\bar{g}_B)$ has more than one expansion coefficient at the two-loop level, which is necessary for the existence of an optimum in variational perturbation theory. At the five-loop level, the combination $\eta + \eta_m$ will be used since it seems to converge fastest.

19.5.3 Critical Exponent ω

We begin by calculating the critical exponent ω from the requirement that $g(g_B)$ has a constant strong-coupling limit, implying the vanishing of (19.73) for $g_B \to \infty$. From the expansion (19.76) we obtain a logarithmic derivative (19.73) up to the term g_B^2, so that Eq. (19.69) can be used to find the scaling condition

$$0 = 1 - \frac{1}{4}\frac{\hat{F}_2^2}{2\hat{F}_3 - \hat{F}_2^2}\rho^2. \tag{19.82}$$

This gives

$$\rho = \sqrt{8\hat{F}_3/\hat{F}_2^2 - 4}. \tag{19.83}$$

Since ω must be greater than zero, only the positive square root is physical. With the explicit coefficients F_1, F_2, F_3 of expansion (19.76), this becomes

$$\rho = 2\sqrt{1 + 3\frac{3N+14}{(N+8)^2}\varepsilon}. \tag{19.84}$$

The associated critical exponent $\omega = \varepsilon/(\rho - 1)$ is plotted in Fig. 19.2. It has the ε-expansion

$$\omega = \varepsilon - 3\frac{3N+14}{(N+8)^2}\varepsilon^2 + \dots\ , \tag{19.85}$$

which is also shown in Fig. 19.2, and agrees with the first two terms obtained from renormalization group calculations in Eq. 17.15.

From Eqs. (19.75), (19.74), and (19.69) we obtain for the critical exponent ω a further equation

$$-\frac{\omega}{\varepsilon} - 1 = -\frac{\rho}{\rho - 1} \quad = \quad -\frac{1}{2}\frac{\hat{F}_2^2\,\rho^2}{3\hat{F}_3 - 2\hat{F}_2^2}, \tag{19.86}$$

which is solved by

$$\rho = \frac{1}{2} + \sqrt{\frac{6\hat{F}_3}{\hat{F}_2^2} - \frac{15}{4}}, \tag{19.87}$$

with the positive sign of the square root ensuring a positive ω. Inserting the coefficients of (19.76), this becomes

$$\rho = \frac{1}{2} + \frac{3}{2}\sqrt{1 + 4\frac{3N+14}{(N+8)^2}\varepsilon}. \tag{19.88}$$

The associated critical exponent $\omega = \varepsilon/(\rho - 1)$ has the same ε-expansion (19.85) as the previous approximation (19.84). The full approximation based on (19.88) is indistinguishable from the earlier one in the plot of Fig. 19.2.

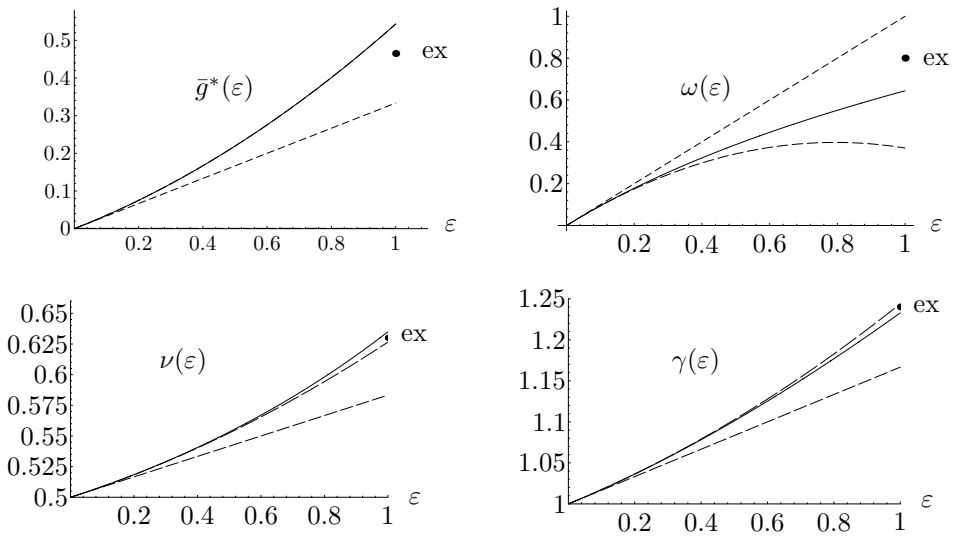

FIGURE 19.2 For Ising universality class ($N = 1$), the first figure shows the renormalized coupling at infinite bare coupling as a function of $\varepsilon = 4 - D$. It is calculated by variational perturbation theory from the first two perturbative expansion terms. The curve coincides with the ε-expansion up to order ε^2. Dashed curves indicate linear and quadratic ε-expansions. The other figures show similarly the critical exponents ω, ν, and γ. The dots mark currently accepted values of $\bar{g}^* \approx 0.466 \pm 0.003$, $\omega \approx 0.802 \pm 0.003$, $\nu = 0.630 \pm 0.002$, and $\gamma = 1.241 \pm 0.004$ obtained from the six-loop calculations in Section 20.2.

Having determined ω, we can now calculate $\bar{g}^*$. Identifying the first three coefficients in the expansion (19.76) with f_0, f_1, f_2 in (19.69) we obtain

$$\bar{g}_2^* = f_0 - \frac{1}{4}\frac{f_1^2}{f_2}\rho^2. \tag{19.89}$$

With (19.84), this reads explicitly

$$\bar{g}_2^* = \frac{3}{N+8}\varepsilon + 9\frac{3N+14}{(N+8)^3}\varepsilon^2, \tag{19.90}$$

which is precisely the well-known ε-expansion of $\bar{g}^*$ in renormalization group calculations up to the second order. Including the next coefficient, we can use formula (19.70) to calculate the next approximation $\bar{g}_3^*$. At $\varepsilon = 1$, the square root turns out to be imaginary, so that it has to be omitted (corresponding to the turning point as optimum). The resulting curve lies slightly ($\approx 8\%$) above the curve (19.90), i.e., represents a worse approximation than (19.90). Indeed, the ε^3-term in $\bar{g}_3^*$ is $81(3N+14)^2/8(N+8)^5$ and disagrees in sign with the exact term $\varepsilon^3[3\,(-33n^3+110n^2+1760n+4544)\,/8\,-36\zeta(3)(N+8)\,(5N+22)]/(N+8)^5$, which we would find by calculating ρ from an expansion (19.76) with one more power in g_B.

19.5.4 Critical Exponent ν

We now turn to the critical exponent ν. Taking the expansion (19.79) to infinite couplings $\bar{g}_B$, we obtain from formula (19.69) the limiting value

$$\eta_m = \frac{\varepsilon}{4}\frac{N+2}{N+8+5\varepsilon/2}\rho^2. \tag{19.91}$$

The corresponding exponent ν is plotted in Fig. 19.2. With the approximation (19.84) for ρ we find for ν the ε-expansion

$$\nu = \frac{1}{2} + \frac{1}{4}\frac{N+2}{N+8}\varepsilon + \frac{(N+2)(N+3)(N+20)}{8(N+8)^3}\varepsilon^2 + \dots \,, \tag{19.92}$$

which is also shown in Fig. 19.2 and agrees with renormalization group results to this order.

19.5.5 Critical Exponent γ

As a third independent critical exponent we calculate the critical exponent of the susceptibility $\gamma = \nu(2-\eta) = (2-\eta)/(2-\eta_m)$ by inserting the coefficients of the expansion (19.81) into formula (19.69), which yields

$$\gamma = 1 + \frac{\varepsilon}{8}\frac{N+2}{N+8-(N-4)\varepsilon/2}\rho^2, \tag{19.93}$$

plotted in Fig. 19.2. This has an ε-expansion

$$\gamma = 1 + \frac{1}{2}\frac{N+2}{N+8}\varepsilon + \frac{1}{4}\frac{(N+2)(N^2+22N+52)}{(N+8)^3}\varepsilon^2 + \dots \,, \tag{19.94}$$

shown again in Fig. 19.2 and agreeing with renormalization group results to this order. The full approximation is plotted in Fig. 19.2. The critical exponent $\eta = 2 - \gamma/\nu$ has the ε-expansion $\eta = (N+2)\varepsilon^2/2(N+8)^2 + \dots$.

Thus we see that variational strong-coupling theory can easily be applied to ϕ^4-theories in $D = 4-\varepsilon$ dimensions and yields resummed expressions for the ε-dependence of all critical exponents. Their ε-expansions agree with those obtained from renormalization group calculations in Chapter 17.

19.6 Three-Loop Resummation

The three-loop calculations are algebraically more involved [12]. Fortunately, the optima of the variational expressions turn out to be determined by turning points, i.e., by the vanishing of the second derivative. At the three-loop order, this implies that the parameter r in (19.70) is zero, thus leading to the three-loop strong-coupling limit (19.71). It is this feature which renders the calculation analytically manageable, involving only a cubic equation for the determination of ρ (for $r \neq 0$, we would have to solve an eight-order equation). In order to obtain ω to three loops, we apply (19.71) to the logarithmic derivative of the three-loop part of (15.18), and find for ρ the following trigonometric representation of the relevant cubic root:

$$\rho = -\frac{1}{6} + \frac{256}{3}a_0\left[106 + N(N+25)\right]^2 - a_0 b_0 \cos\left(\frac{-2\pi+\theta}{3}\right). \tag{19.95}$$

The angle θ and the constants $a_0\, b_0$ are given by

$$\theta = \arccos\left(\frac{\left[13776 + 4738N + N^2(8N+405) + 96(5N+22)\zeta(3)\right]^2}{2\left[106+N(N+28)\right]\left\{(N+8)\left[13776+4738N+N^2(8N+405)+96(5N+22)\zeta(3)\right]\right\}^{3/2}}\right.$$
$$\left.\times \frac{1}{\left[2209664 + 1040160N + 162982N^2 + 9683N^3 + 184N^4 + 672(N+8)(5N+22)\zeta(3)\right]^{3/2}}\right)$$

$$\times \Big\{ 67181166592 + 64001040384N + 25893312000N^2 + 5641828480N^3 + 713027988N^4 + 54733044N^5 + 2760157N^6 + 88332N^7 + 1440N^8 - 192(N+8)(5N+22)\left[4084864 + 1952480N + 323706N^2 + 20021N^3 + 514N^4\right]\zeta(3) + 746496\left[(N+8)(5N+22)\zeta(3)\right]^2 \Big\}\Big), \tag{19.96}$$

$$a_0 = \left[446336 + 213280N + 35334N^2 + 2179N^3 + 56N^4 - 864(N+8)(5N+22)\zeta(3)\right]^{-1} \tag{19.97}$$

$$b_0 = 3\sqrt{(N+8)\left[13776 + 4738N + N^2(8N+405) + 96(5N+22)\zeta(3)\right]} \times \sqrt{2209664 + 1040160N + 162982N^2 + 9683N^3 + 184N^4 + 672(N+8)(5N+22)\zeta(3)}. \tag{19.98}$$

To save space, we have written down the solution directly for $\varepsilon = 1$. For the physically interesting cases $N = 0, \ldots, 4$, we obtain the values for $D = 3$ dimensions shown in Table 19.2 . Figure 19.3 illustrates the two- and three-loop critical exponent of the approach to scaling $\omega = \varepsilon/(\rho - 1)$ as a function of N.

TABLE 19.2 Critical exponent ω from three-loop strong-coupling theory in $4 - \varepsilon$ dimensions.

N	0	1	2	3	4
ρ	2.41829	2.40384	2.38683	2.36910	2.35157
ω	0.705073	0.712332	0.721069	0.730405	0.73988

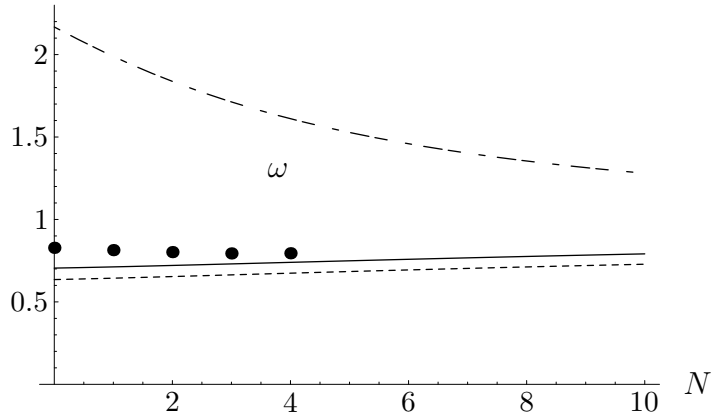

FIGURE 19.3 Two-loop (short-dashed) and three-loop (solid) critical exponent ω for different O(N)-symmetries. The ε-expansion (mixed-dashed) and the six and seven loops theoretical results to be listed in Tables 20.1 and 20.2 (dots) are displayed for comparison.

Given ρ, we can determine the other exponents. The results are

$$\gamma = 1 - \frac{\varepsilon(N+2)\left[\varepsilon(N-4) - 2(N+8)\right]\rho(\rho+1)(2\rho-1)}{3\left[8(N+8)^2 - 4\varepsilon(2N^2 - N - 106) + \varepsilon^2(2N^2 + 17N + 194)\right]} + \frac{8\varepsilon(N+2)\left[\varepsilon(N-4) - 2(N+8)\right]^3(2\rho-1)^3}{27\left[8(N+8)^2 - 4\varepsilon(2N^2 - N - 106) + \varepsilon^2(2N^2 + 17N + 194)\right]^2}, \tag{19.99}$$

$$\nu = \frac{1}{2} - \frac{\varepsilon(N+2)\left[\varepsilon(N-3) - 2(N+8)\right]\rho(\rho+1)(2\rho-1)}{12\left[4(N+8)^2 - 2\varepsilon(2N^2 + N - 90) + \varepsilon^2(N^2 + 9N + 95)\right]}$$

$$+\frac{\varepsilon(N+2)\left[\varepsilon(N-3)-2(N+8)\right]^3(2\rho-1)^3}{27\left[4(N+8)^2-2\varepsilon(2N^2+N-90)+\varepsilon^2(N^2+9N+95)\right]^2}. \tag{19.100}$$

Figures 19.4 and 19.5 illustrate the accuracy of the two- and three-loop critical exponents γ and ν as a function of N.

If we keep ε in (19.95)–(19.98), we obtain

$$\rho = 2+\frac{3(3N+14)}{(N+8)^2}\varepsilon-\frac{96\zeta(3)(5N+22)(N+8)+33N^3+214N^2+1264N+2512}{4(N+8)^4}\varepsilon^2. \tag{19.101}$$

Reexpanding the combination $\omega=\varepsilon/(\rho-1)$ in powers of ε up to ε^3, we rederive the corresponding terms in the ε-expansion (17.15). Inserting this expansion into ρ, we would have recovered the three-loop parts of the ε-expansions for γ and η of Eqs. (17.13) and (17.14) [recalling $\gamma=\nu(2-\eta)$]. The critical exponent η is obtained using $2-\gamma/\nu$, with γ and ν from (19.99)

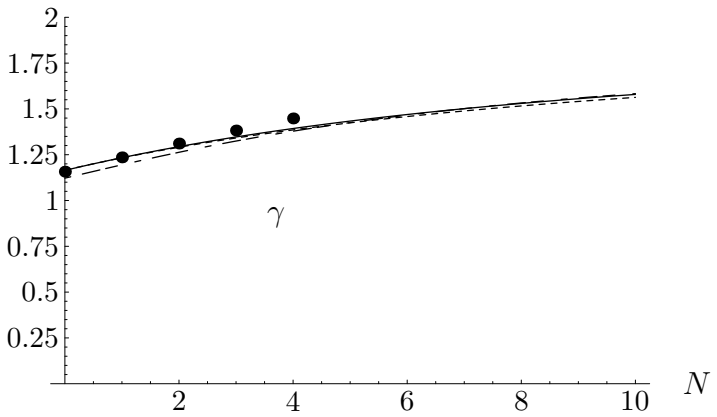

FIGURE 19.4 Two-loop (short-dashed) and three-loop (solid) critical exponent γ. For comparison, we also show the ε-expansion (mixed-dashed) and the theoretical values of Tables 20.1 and 20.2 (dots).

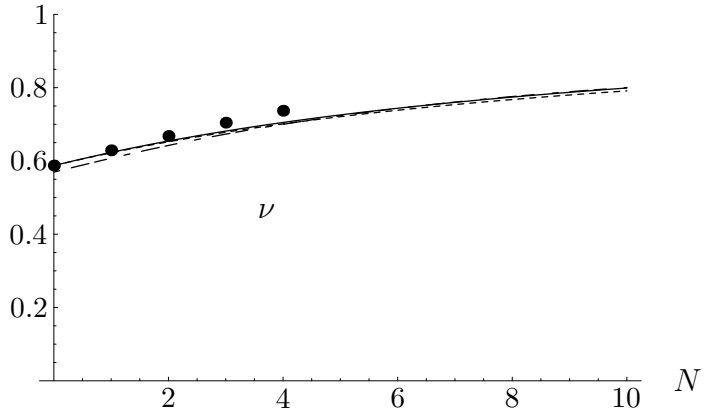

FIGURE 19.5 Two-loop (short-dashed) and three-loop (solid) critical exponent ν. For comparison, we also show the ε-expansion (mixed-dashed) and the theoretical values of Tables 20.1 and 20.2 (dots).

and (19.100), respectively. From this we can recover the ε-expansion (17.13).

Let us also calculate directly the strong-coupling limit of η from the three-loop extension of (19.80):

$$\eta(\bar{g}_B)=\frac{N+2}{18}\bar{g}_B^2-\frac{(N+2)(N+8)}{216}\left(1+\frac{8}{\varepsilon}\right)\bar{g}_B^3+\dots\ . \tag{19.102}$$

Since the linear term is absent, the optimum of variational perturbation theory is given by an extremum in which the root r in (19.70) is equal to -1, the optimum lying at $\bar{g}_B = -2\bar{f}_2/(3f_3)$, so that

$$\eta = \frac{4}{27}\frac{\bar{f}_2^3}{f_3^2} = \frac{32}{27}\frac{(2\rho-1)^3(N+2)}{(N+8)^2(8+\varepsilon)^2}\varepsilon^2. \tag{19.103}$$

With the three-loop ε-expansion (19.101) for ρ, this leads again to the correct terms in ε-expansion (17.13) for η. The difference between $\eta = 2-\gamma/\nu$ and (19.103) at $\varepsilon = 1$ is illustrated in Figure 19.6 which also shows a direct plot of the ε-expansion for η as well as the theoretical values quoted in Tables 20.1 and 20.2 . In this case, the ε-expansion happens to yield the best critical exponent η, followed by the strong-coupling limit of the direct series (19.103). Comparing the different results, we see that they differ by about 30%. This is due to the smallness of η. Compared to unity, the error is small.

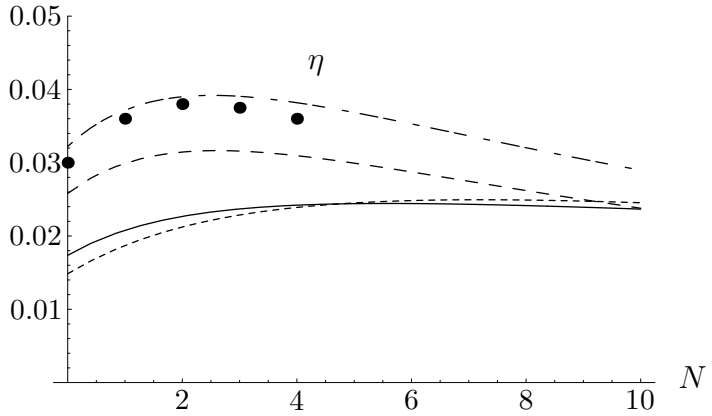

FIGURE 19.6 Two-loop (short-dashed) and three-loop (solid) critical exponent η from the definition $2-\gamma/\nu$. For comparison, we also show the ε-expansion (short- and long-dashed), η from the strong-coupling limit of the direct (medium-dashed) series (19.103) and the theoretical values of Tables 20.1 and 20.2 (dots).

Let us finally calculate the critical exponent η_m up to three loops. The extension of the perturbation series (19.79) up to three loops reads

$$\begin{aligned}\eta_m(\bar{g}_B) &= \frac{N+2}{3}\bar{g}_B - \frac{N+2}{18}\left(5+2\frac{N+8}{\varepsilon}\right)\bar{g}_B^2 + \frac{N+2}{108}\left[3\,(5N+37)\right.\\ &+ \left.\frac{2\,(19N+122)}{\varepsilon} + \frac{4\,(N+8)^2}{\varepsilon^2}\right]\bar{g}_B^3 + \dots\ .\end{aligned} \tag{19.104}$$

From this we obtain the strong-coupling limit

$$\begin{aligned}\eta_m &= \frac{\varepsilon(N+2)(2N+16+5\varepsilon)\rho(\rho+1)(2\rho-1)}{3\left[4(N+8)^2+\varepsilon(38N+244)+3\varepsilon^2(5N+37)\right]}\\ &- \frac{4\varepsilon(N+2)(2N+16+5\varepsilon)^3(2\rho-1)^3}{27\left[4(N+8)^2+\varepsilon(38N+244)+3\varepsilon^2(5N+37)\right]^2}.\end{aligned} \tag{19.105}$$

This result is analytically different from that obtained from (19.100) via the scaling relation $\eta_m = 2-\nu^{-1}$. Numerically, however, it is close to it, as can be seen in Figure 19.7. For comparison, the figure also shows plots of the ε-expansion (19.106), and the theoretical values of Tables 20.1 and 20.2 .

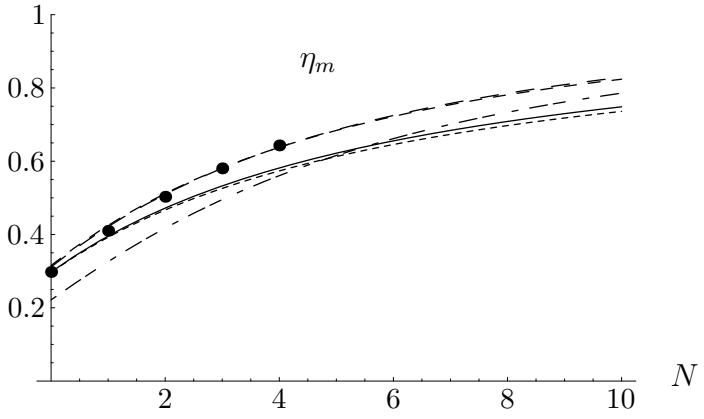

FIGURE 19.7 Two-loop (short-dashed) and three-loop (solid) critical exponent η_m from the definition $2-\nu^{-1}$. For comparison, we also show the ε-expansion (short- and long-dashed), η_m from the strong-coupling limit of the direct two-loop (medium-dashed) and three-loop (long-dashed) series and the theoretical values of Tables 20.1 and 20.2 (dots).

Inserting into (19.105) the ε-expansion (19.101) for ρ, we find

$$\begin{aligned}\eta_m &= \frac{N+2}{N+8}\varepsilon + \frac{(N+2)(13N+44)}{2(N+8)^3}\varepsilon^2 \\ &+ \frac{(N+2)\left[5312+2672N+452N^2-3N^3-96(N+8)(5N+22)\zeta(3)\right]}{8(N+8)^5}\varepsilon^3. \quad (19.106)\end{aligned}$$

For completeness, we list some numeric values of the critical exponents up to three loops in Table 19.3 .

TABLE 19.3 Critical exponents ν, η_m, η from three-loop strong-coupling theory in $4-\varepsilon$ dimensions.

N	0	1	2	3	4
γ	1.16455	1.2338	1.29426	1.34697	1.39307
ν	0.587376	0.623381	0.654552	0.681561	0.705071
η_m	0.311607	0.421796	0.509799	0.580684	0.638337
η	0.0258218	0.029917	0.031452	0.0315846	0.03096

19.7 Five-Loop Resummation

The calculations in the last section have illustrated the power of the variational procedure, but do not yet give good results for the critical exponents. In order to achieve higher accuracy, we have to go to five loops in a straightforward extension of the two-loop treatment[13].

19.7.1 Critical Exponent ω

As in the two-loop calculations of the last section, we start by resumming the logarithmic derivative of $\bar{g}(\bar{g}_B)$ to determine the critical exponent ω of the approach to scaling.

As in Subsection 19.5.3, the exponent ω is determined by identifying the perturbation expansions of $\bar{g}(\bar{g}_B)$, truncated as in (19.53), with the function W_L in Eq. (19.54), and requiring that the theory scales as observed experimentally. This implies that $\bar{g}(\bar{g}_B)$ approaches a constant in the strong-coupling limit. The ratio of powers p/q on the left-hand side of (19.54) must therefore be zero. The expansion of the logarithmic derivative of $\bar{g}(\bar{g}_B)$ is calculated as indicated in Eq. (19.73) for a function $F(\bar{g}_B) = \bar{g}(\bar{g}_B)$. By Eq. (19.54) [or (19.61)], the resulting function $f(\bar{g}_B)$ has to be equal to $p/q = s$ in the strong-coupling limit, i.e., equal to zero.

Instead of the two-loop expansion for $\bar{g}(\bar{g}_B)$ in (19.76), we use the five-loop expansion in (15.18). Thus we obtain for $\rho = 1 + q/2 = 1 + \varepsilon/\omega$ higher L-loop approximations ρ_L. Altogether, we find four approximations ω_L to the approach parameter $\omega = 2/q = \varepsilon/(\rho - 1)$, with $L = 2, 3, 4, 5$. As a check we perform their ε-expansions and find that they agree with the initial ε-expansion (17.15) derived, in the renormalization group approach, from the derivative of the β-function at the fixed point.

Our variational expressions are evaluated without an ε-expansion at $\varepsilon = 1$. In Fig. 19.8, the resulting L-loop approximations ω_L are plotted as functions of L. The ω_L-values are obviously

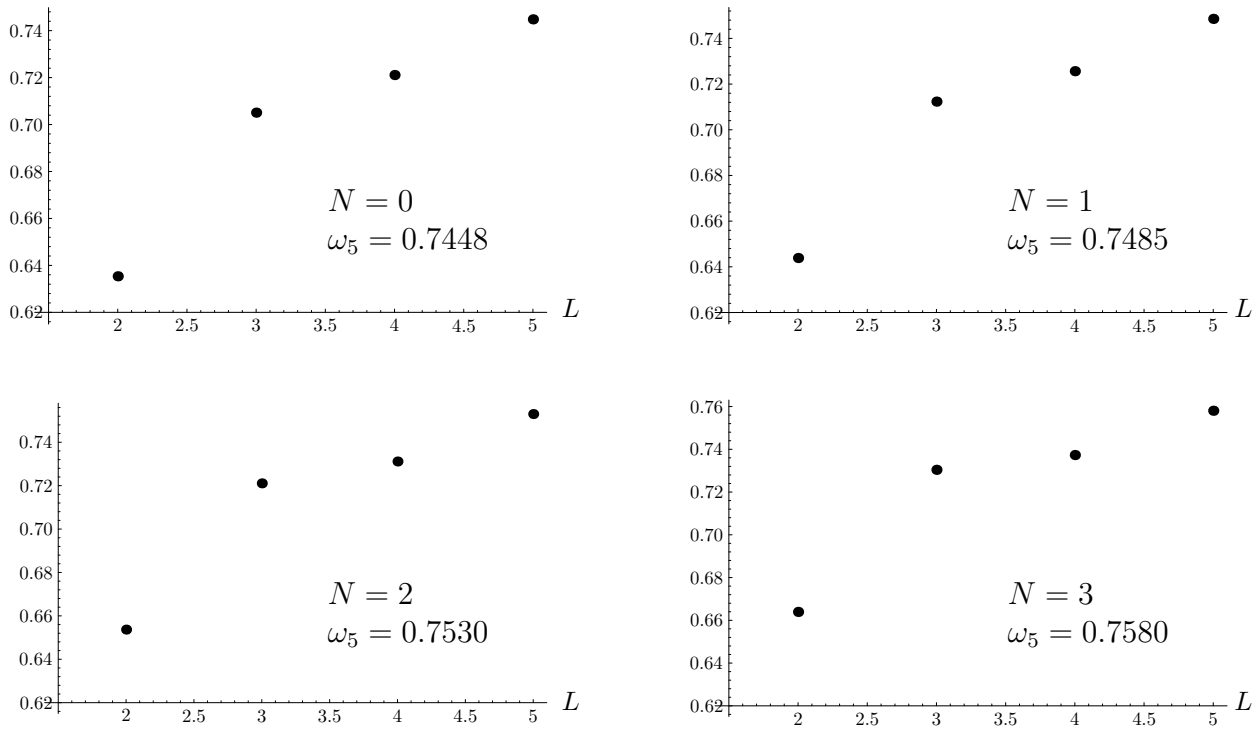

FIGURE 19.8 Critical exponent of approach ω calculated from $f_L^* = s_L^* = 0$, plotted against the order of approximation L.

not yet asymptotic, calling for an extrapolation to infinite L. This is possible with the help of the theoretical knowledge on the L-dependence of the strong-coupling limit as determined in Eq. (19.51). For an arbitrary function $f(\bar{g}_B)$ with a constant strong-coupling limit approachad as in Eq. (19.66), the L-dependence is of the form

$$f_L^* \propto f^* + \text{const} \times \mathrm{e}^{-c\,L^{1-\omega}}. \tag{19.107}$$

The extrapolation to infinite order L may be carried out in two ways. We may choose an ω-value near the suspected correct exponent, and calculate the strong-coupling limits $f_L^* = s_L^*$

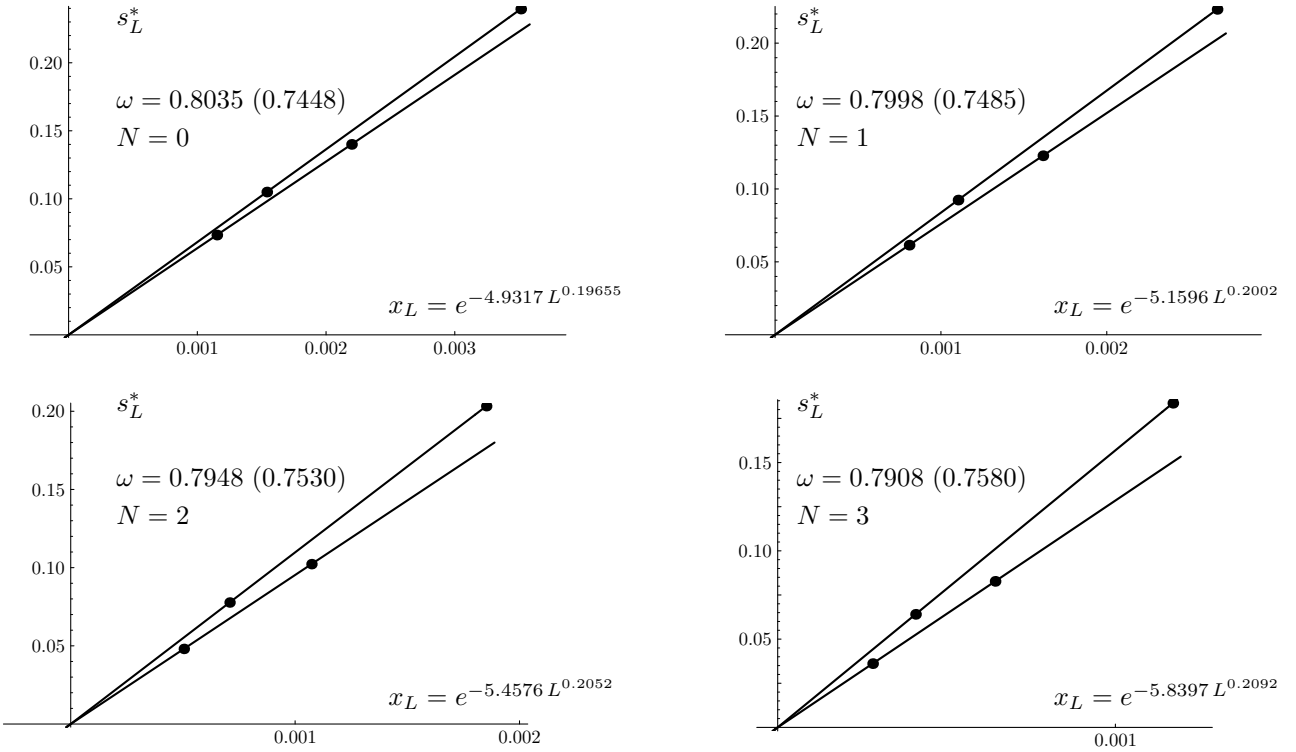

FIGURE 19.9 Approach to zero of the logarithmic derivative $(p/q)_L \equiv s_L^* = f_L^*$ of $\bar{g}(\bar{g}_B)$ as a function of the variable x_L. The critical exponent $\omega = 2/q$ is determined by requiring the straight lines to intersect at $x_L = 0$. Its value is given in the equation. The number in parentheses is the highest approximation ω_6 showing the exptrapolation distance to the final value. Both numbers are listed in Table 19.4 .

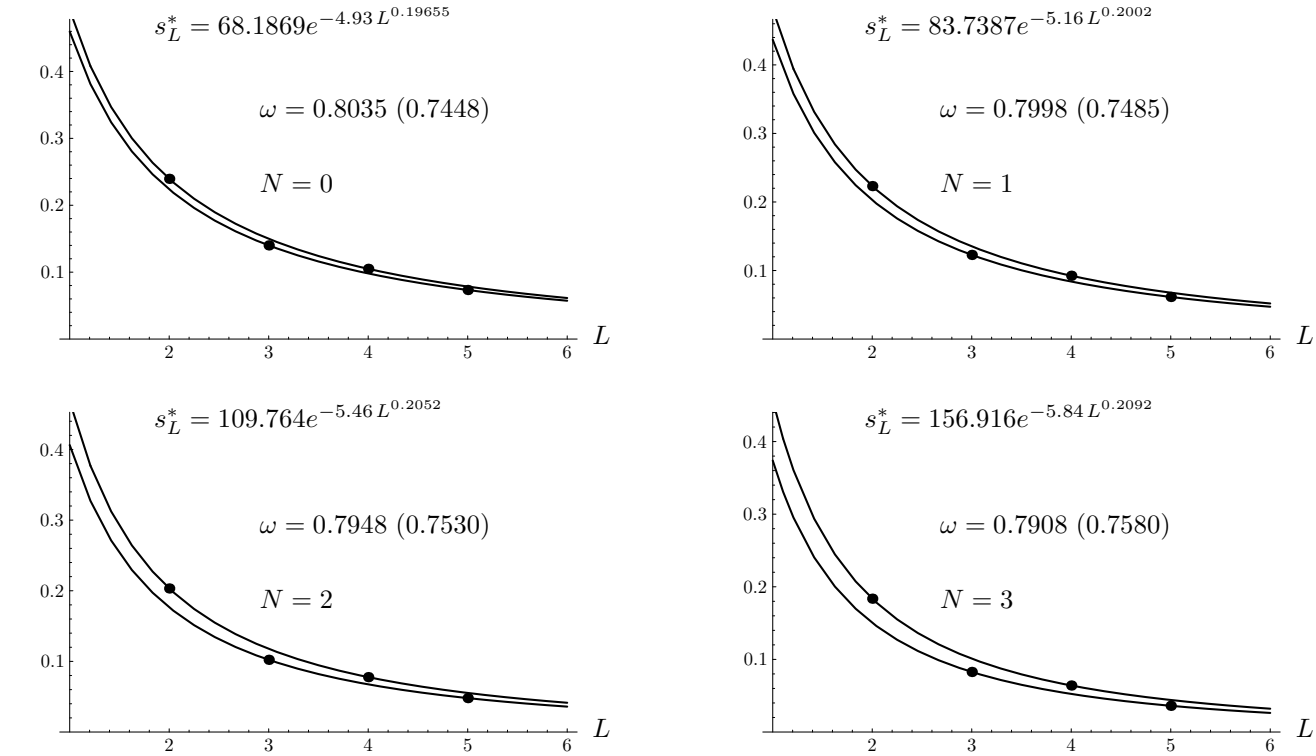

FIGURE 19.10 Same strong-coupling limits of logarithmic derivative of $\bar{g}(\bar{g}_B)$ as in Fig. 19.9, but plotted against the order L of the approximation. The extrapolating functions are written on top of each figure. Ihe extrapolated ω is given in the equation. The number in parentheses is again the highest approximation ω_6 showing the exptrapolation distance to the final value. Both numbers are listed in Table 19.4 .

of the logarithmic derivative of $\bar{g}(\bar{g}_B)$. Through these we fit the theoretical L-behavior (19.107). Then we vary ω and the fit parameter c until the fit approaches as smoothly as possible the limit $s_L^* = 0$ for infinite L.

Alternatively, and apparently more reliably, we plot for a certain ω and c the strong-coupling limits $s_L^* = f_L^*$ against the variable $x_L = \mathrm{e}^{-c\,L^{1-\omega}}$ instead of L. The parameter c is chosen such that the points lie as close as possible on a straight line. Since the points are obtained alternatively from minima and turning points for even and odd approximations, respectively, they are expected to lie on slightly different straight lines. We determine c by requiring these lines to cross at $x_L = 0$. With this condition, the two lines yield the same value for $s^* = s_\infty$. The trial ω is then varied until s^* is equal to zero. The final plots are shown in Fig. 19.9. For comparison, we also show the corresponding direct plots against the order L of the approximation in Fig. 19.10.

Table 19.4 lists in the first column the calculated values of ω for infinite L and $N = 0, 1, 2, 3$. The number in parentheses is the value ω_5 determined from the condition $s_5^* = f_5^* = 0$. It shows the importance of the extrapolation.

The extrapolated values for ω are now used to construct the strong-coupling limits for the exponents ν, γ and η.

19.7.2 Critical Exponent ν

For ν, we can proceed as in Eq. (19.91) of the last section, calculating the strong-coupling limit of $\eta_m(\bar{g}_B)$. Its perturbation expansion $\eta_m(\bar{g}_B) = 2\gamma_m(\bar{g}_B)$ is found by inserting (15.18) into (17.7). The critical exponents ν are obtained from the strong-coupling limits of η_m via the scaling relation $\nu = 1/(2 - \eta_m)$. The resulting exponents are shown in Table 19.4 as ν(II).

Alternatively, we apply the procedure to the series $\nu(\bar{g}_B)$, and find directly the strong-coupling limits of the exponent ν as shown in Table 19.4 as ν(I).

In both cases, the extrapolation to infinite order proceeds as before. We use again a function of the form (19.107) to extrapolate the results for $L = 2, 3, 4, 5$ to infinite L. The results are shown in Figs. 19.11 and 19.12 for the direct calculation of ν. The horizontal lines indicate the limit $L \to \infty$. The extrapolating functions are displayed on top of each figure. The results of these calculations are listed in Table 19.4 . The value $\nu = 0.6697$ for $N = 2$ corresponds to a critical exponent

$$\alpha = 2 - 3\nu \approx -0.0091, \tag{19.108}$$

which is in satisfactory agreement with the experimental space shuttle value -0.01056 ± 0.0004 in Eq. (1.23)

All results depend on the value of ω used for the resummation. Let us estimate the error resulting from errors in ω. This is done by calculating ν for two adjacent ω-values, and we find

$$\Delta\nu = \left\{ \begin{array}{l} -0.0900 \times (\omega - 0.8035) \\ -0.1375 \times (\omega - 0.7998) \\ -0.1853 \times (\omega - 0.7948) \\ -0.2271 \times (\omega - 0.7908) \end{array} \right\} \quad \text{for} \quad \left\{ \begin{array}{l} N = 0 \\ N = 1 \\ N = 2 \\ N = 3 \end{array} \right\}. \tag{19.109}$$

19.7.3 Critical Exponent η and γ

The calculation of the exponent η is always difficult, since its perturbation expansion starts out with $\bar{g}_B^2$. Thus we find only three approximants η_3, η_4, η_5, and these are not sufficient to

ω	Var.-Pert.	Borel-Res. (GZ)	Chapter 17
	$\omega\,(\omega_5)$		
$N=0$	0.8035(0.7448)	0.828 ± 0.023	0.817 ± 0.021
$N=1$	0.7998(0.7485)	0.814 ± 0.018	0.806 ± 0.013
$N=2$	0.7948(0.7530)	0.802 ± 0.018	0.800 ± 0.013
$N=3$	0.7908(0.7580)	0.794 ± 0.018	0.796 ± 0.011

ν	Var.-Pert.		Borel-Res. (GZ)	Chapter 17
	$\nu\,(\nu_5)$ (I)	$\nu\,(\nu_5)$ (II)		
$N=0$	0.5874(0.5809)	0.5878(0.5832)	0.5875 ± 0.0018	0.5865 ± 0.0013
$N=1$	0.6292(0.6171)	0.6294(0.6222)	0.6293 ± 0.0026	0.6268 ± 0.0022
$N=2$	0.6697(0.6509)	0.6692(0.6597)	0.6685 ± 0.0040	0.6642 ± 0.0111
$N=3$	0.7081(0.6821)	0.7063(0.6951)	0.7050 ± 0.0055	0.6987 ± 0.0051

η	Var.-Pert.		Borel-Res. (GZ)	Chapter 17
	$\eta\,(\eta_5)$ (I)	$\eta\,(\eta_5)$ (II)		
$N=0$	0.0316(0.0234)	0.0305(0.0234)	0.0300 ± 0.0060	0.0344 ± 0.0042
$N=1$	0.0373(0.0308)	0.0367(0.0308)	0.0360 ± 0.0060	0.0395 ± 0.0043
$N=2$	0.0396(0.0365)	0.0396(0.0365)	0.0385 ± 0.0065	0.0412 ± 0.0041
$N=3$	0.0367(0.0409)	0.0402(0.0409)	0.0380 ± 0.0060	0.0366 ± 0.0020

γ	Var.-Pert.	Borel-Res. (GZ)
	$\gamma\,(\gamma_5)$	
$N=0$	1.1576(1.1503)	1.1575 ± 0.0050
$N=1$	1.2349(1.2194)	1.2360 ± 0.0040
$N=2$	1.3105(1.2846)	1.3120 ± 0.0085
$N=3$	1.3830(1.3452)	1.3830 ± 0.0135

TABLE 19.4 Extrapolated critical exponents from five-loop ε-expansions, compared with results of Chapter 17 and of Guida and Zinn-Justin (GZ), which agree with our present numbers. The difference between the versions (I) and (II) of the exponents ν and η are explained in the text. The numbers in parentheses are the six-loop approximations showing the exptrapolation distance to the final values.

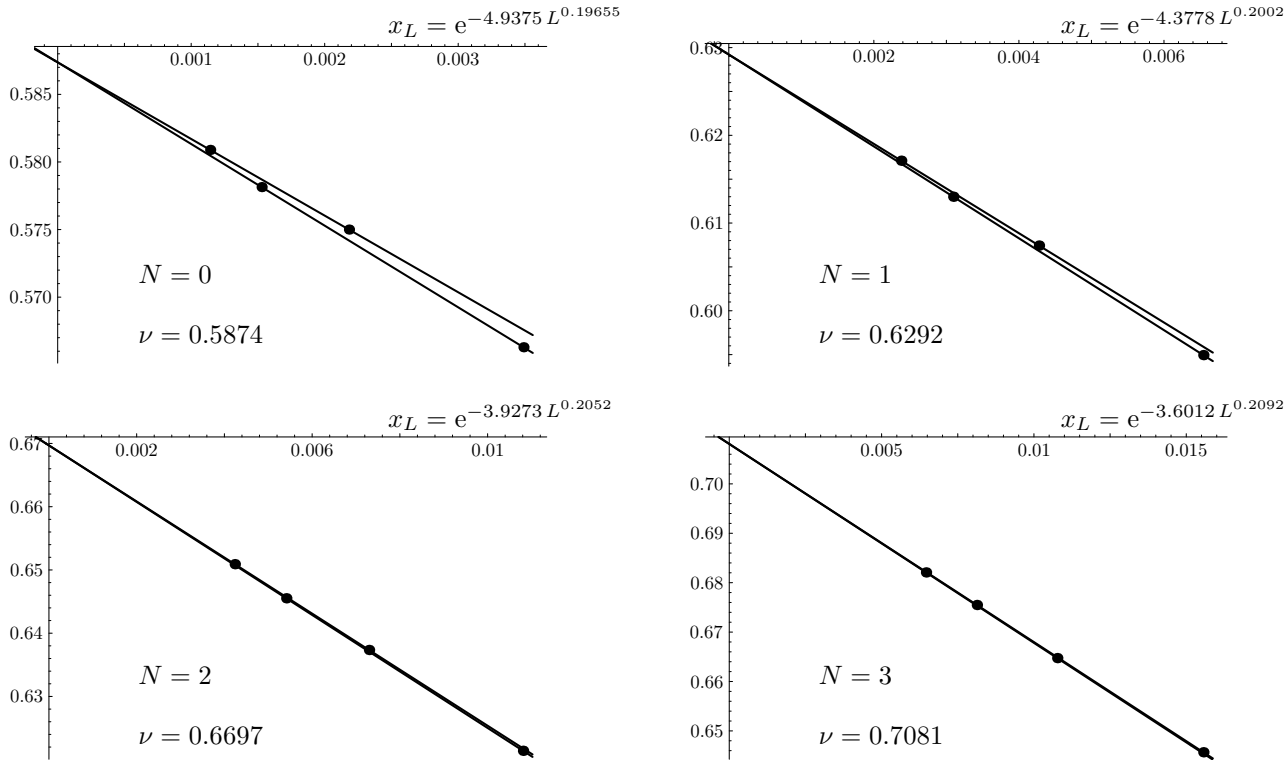

FIGURE 19.11 Critical exponent ν(I) from variational perturbation theory, plotted as a function of x_L. Requiring the lines to cross at $x_L = 0$ determines the parameter c in x_L. See the description of the fitting procedure in the text and the final values in Table 19.4 .

carry out a reliable extrapolation procedure. In order to circumvent this, we study the strong-coupling limit of $\eta_m(\bar{g}_B) + \eta(\bar{g}_B)$, and subtract from this the strong-coupling limit of $\eta_m(\bar{g}_B)$. This is derived from $\eta_m = 2 - \nu^{-1}$ with either the values ν(I) or ν(II) of Table 19.4 . The results are called η(I) and η(II), respectively, and shown in Figs. 19.13 and 19.14. The horizontal line marks the limit $L \to \infty$. The extrapolating function is plotted on top of the figure.

We may calculate η also from another independent strong-coupling limit using the perturbation expansion for the critical exponent $\gamma = \nu(2 - \eta)$. The extrapolation for this exponent is shown in Figs. 19.15 and in 19.16. The resulting values for γ are also listed in Table 19.4 . The dependence on the value of ω is in the same order of magnitude as in the case of ν:

$$\Delta\gamma = \left\{ \begin{array}{l} -0.1500 \times (\omega - 0.8035) \\ -0.2237 \times (\omega - 0.7998) \\ -0.3147 \times (\omega - 0.7948) \\ -0.4014 \times (\omega - 0.7908) \end{array} \right\} \quad \text{for} \quad \left\{ \begin{array}{l} N = 0 \\ N = 1 \\ N = 2 \\ N = 3 \end{array} \right\}. \tag{19.110}$$

Table 19.4 contains the results of the extrapolation to infinite order followed in parentheses by the 5th-order approximation. For comparison with the results of other methods, see Table 20.1 in the next chapter. Here, we only append the earlier results of the resummation of the ε-expansion in Chapter 17, and those of Guida and Zinn-Justin (GZ) [14]. The present numbers agree well with either of them. The differences between ν(I) and ν(II), and between η(I) and η(II), are much smaller than the errors given in Chapter 17, or in GZ.

It is interesting to note that the results of the strong-coupling theory agree very well with those derived from Borel-resummations, which make use of the known large-order behavior of the perturbation series. So far, the strong-coupling theory does not take advantage of this

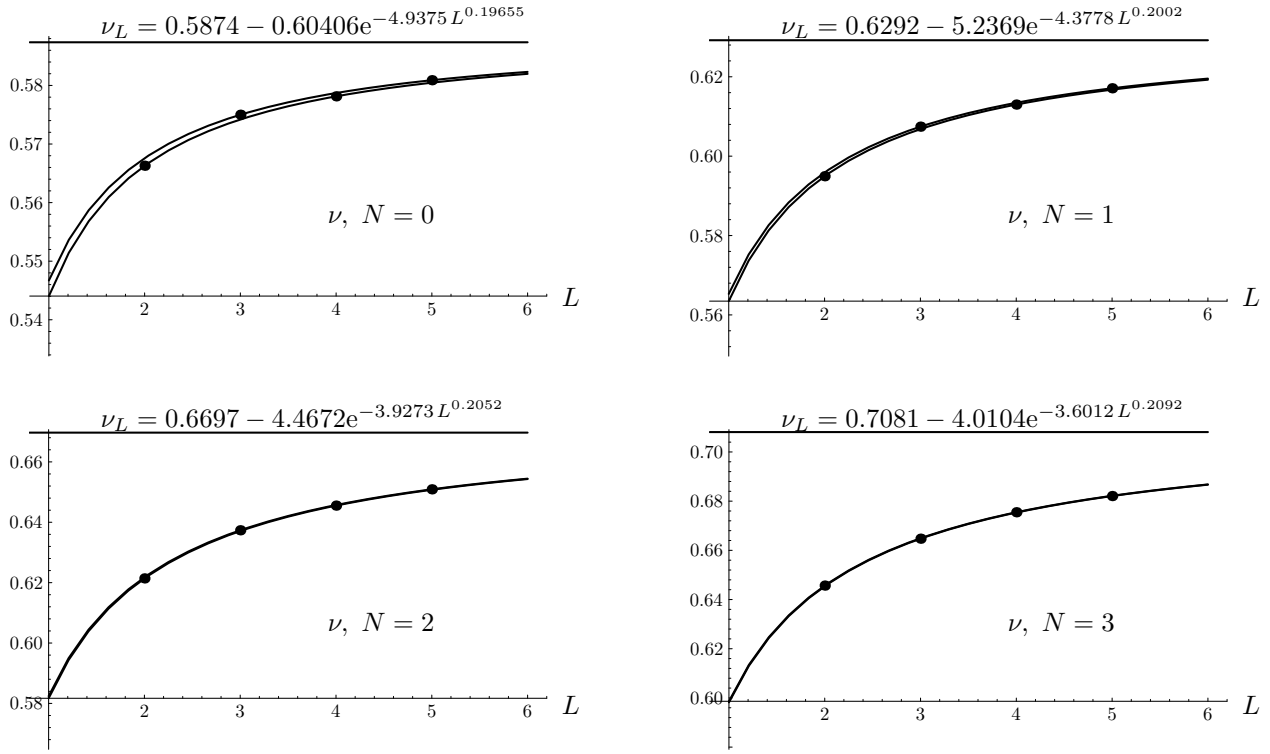

FIGURE 19.12 Critical exponent ν(I) from variational perturbation theory, as a function of the order L of approximation. The full fit function is written on top of the figure. The limiting values are listed in Table 19.4 .

knowledge of the large-order behavior. It compensates for this by incorporating, in an essential way, the approach (19.66) to the strong-coupling limit. Further improvement comes from the theoretical knowledge of the large-L behavior (19.107) of the approximations.

The incorporation of the large-order behavior into the strong-coupling theory will be described in the Chapter 20.

19.8 Interpolating Critical Exponents between Two and Four Dimensions

Knowing the ε-expansions for the critical exponents, the question arises whether these expansions can also be resummed at $\varepsilon = 2$, i.e., in D=2 dimensions. However, with the difficulties encountered in going to $\varepsilon = 1$, we see little hope in obtaining reliable numbers this way.

Fortunately, there exists a completely independent access to the critical exponents ν and η from another field theory, the O(N)-symmetric *nonlinear σ-model*. The *universality hypothesis* of critical phenomena states that all systems with equal Goldstone bosons should have the same critical exponents. Thus renormalization group studies of O(N)-symmetric nonlinear σ-models in $D = 2 + \epsilon$ dimensions at $\epsilon = 1$, should yield the same critical exponents as O(N)-symmetric ϕ^4-theories as long as the second-order character of the transition is not destroyed by unexpected fluctuation effects. These conditions restrict the comparison to $N > 2$.

For $N = 1$ (Ising case), there are no Goldstone bosons, and for $N = 2$ (XY-model), the transition is of infinite order. In this case, the divergence of the correlation length with temperature cannot be parametrized like $\xi \propto |T - T_c|^{-\nu}$, as shown by Kosterlitz and Thouless [15].

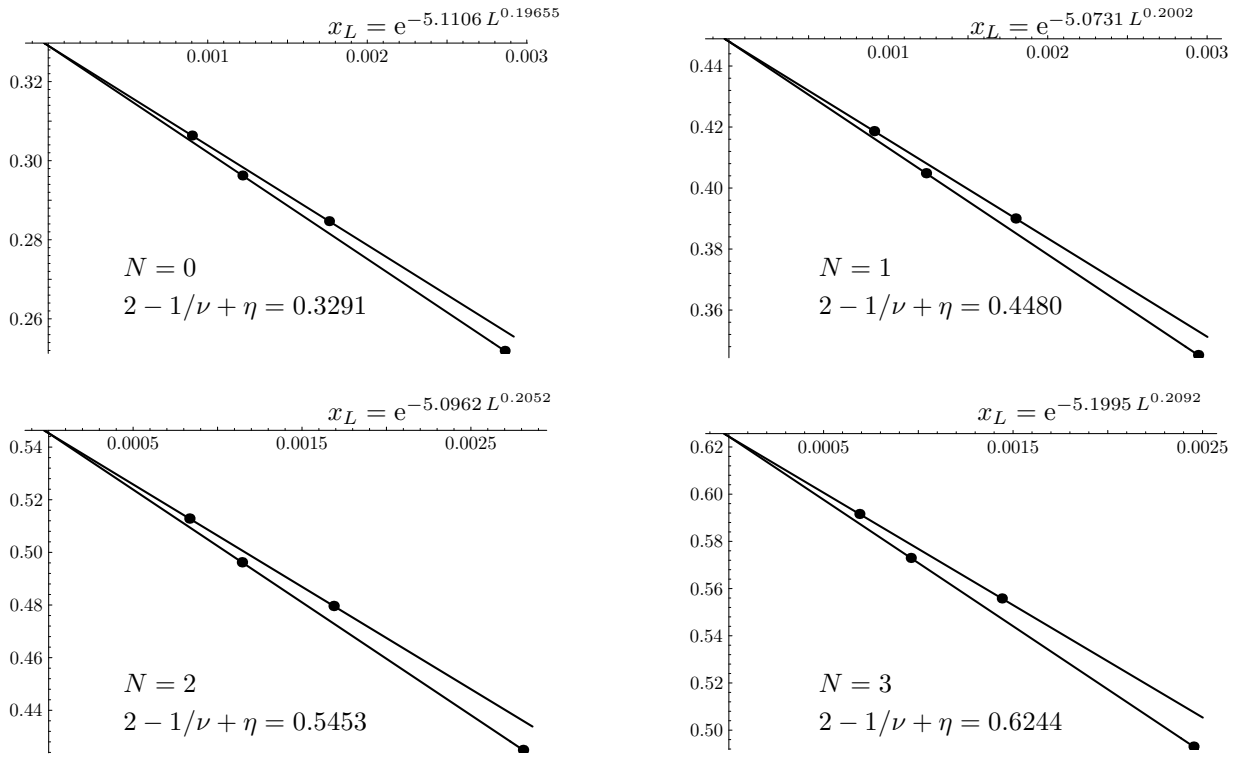

FIGURE 19.13 Determination of critical exponent η from the strong-coupling limit of $\eta_m + \eta$, plotted as a function of x_L. Requiring the lines to cross at $x_L = 0$ determines the parameter c in x_L. See the description of the fitting procedure in the text and the list of limiting values in Table 19.4 .

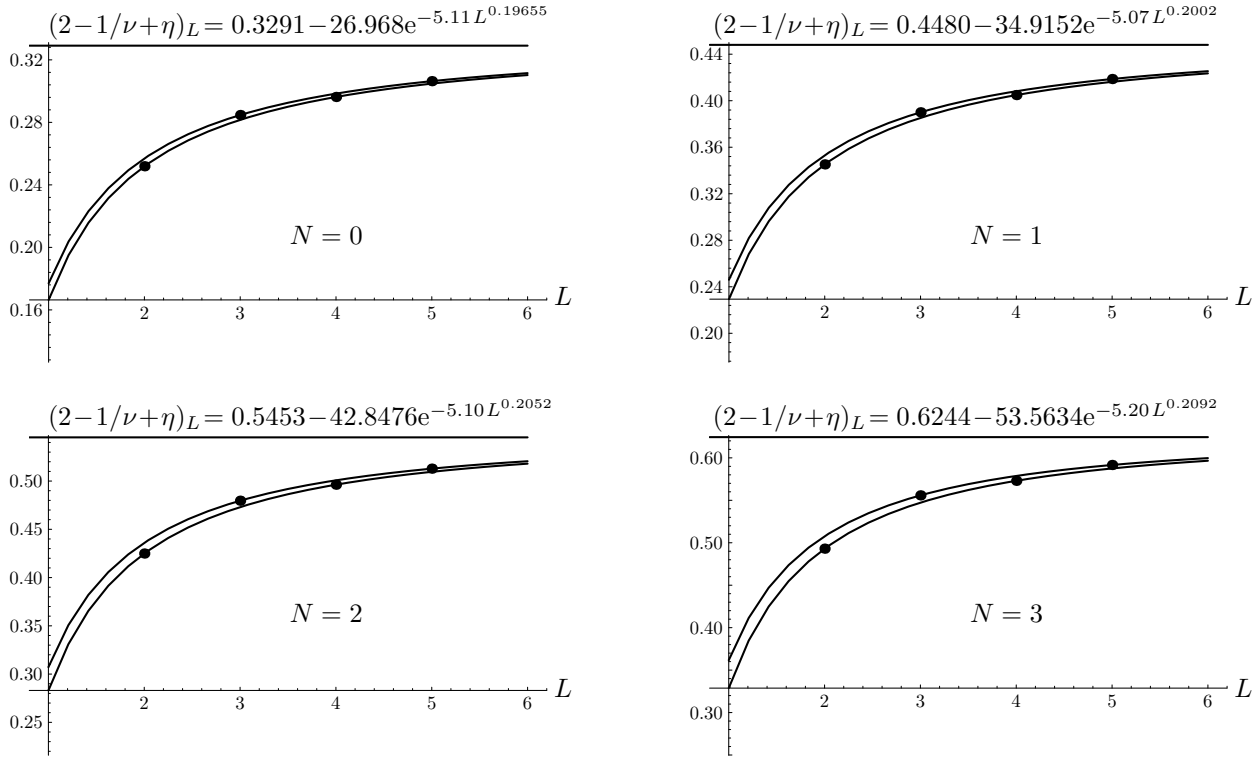

FIGURE 19.14 Same as above, plotted against the order of approximation L. The full fit function is written on top of the figure. The limiting values are listed in Table 19.4 .

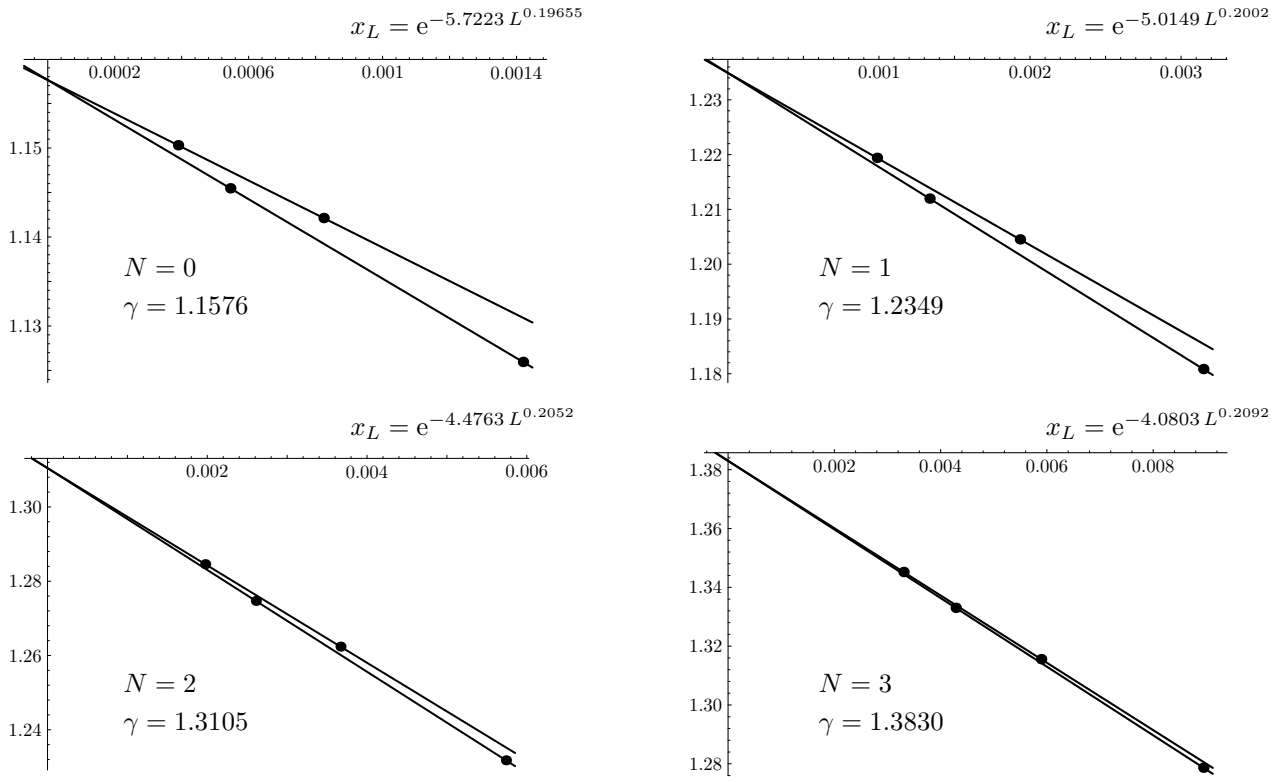

FIGURE 19.15 Critical exponent γ from variational perturbation theory, plotted as a function of x_L. Requiring the lines to cross at $x_L = 0$ determines the parameter c in x_L. See the description of the fitting procedure in the text. The limiting values are listed in Table 19.4 .

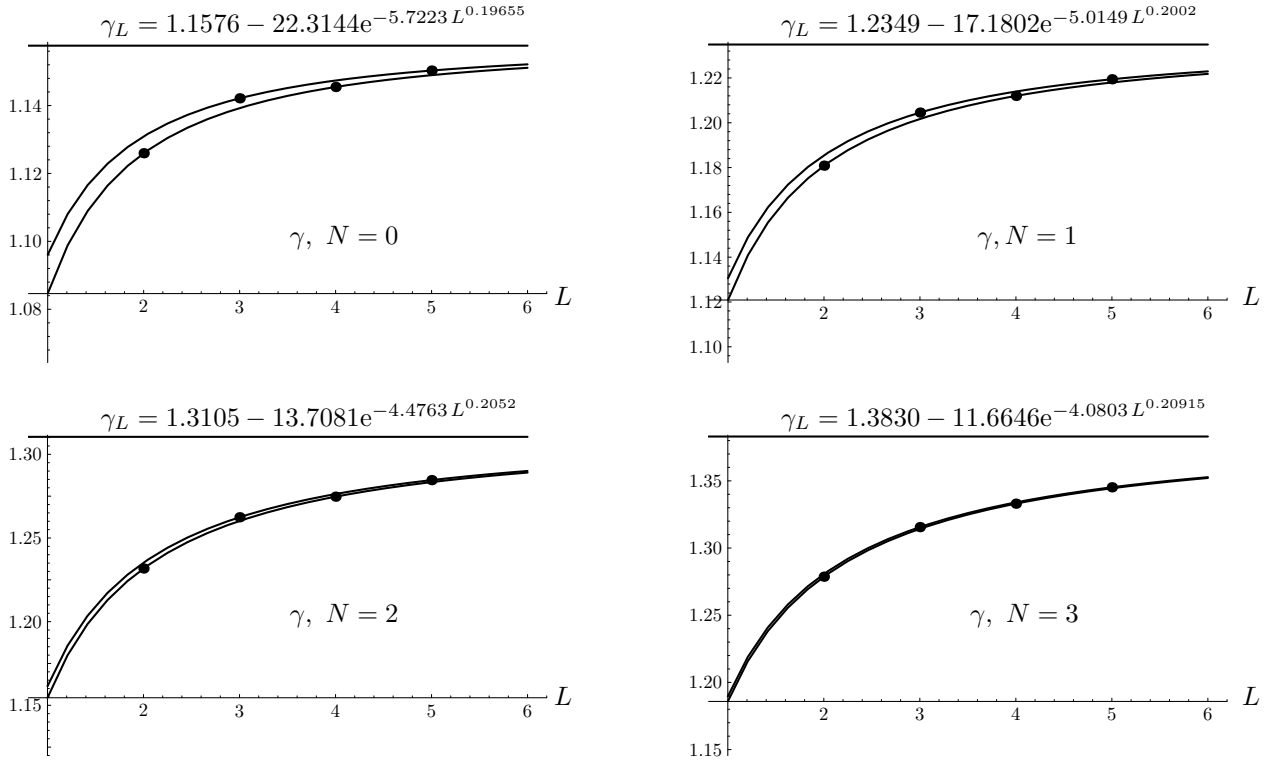

FIGURE 19.16 Critical exponent γ from variational perturbation theory, plotted as a function of the order of approximation L. The full fit function is written on top of the figure. The limiting values are listed in Table 19.4 .

The nonlinear σ-model with the same Goldstone bosons as the ϕ^4 theory for $N > 2$ can be studied in $D = 2+\epsilon$ dimensions and yields expansions for the critical exponents in powers of ϵ. Note the distinct notation of ε in $D = 4-\varepsilon$ and ϵ in $D = 2+\epsilon$. Up to now, the latter expansions have remained rather useless for any practical calculation owing to their non-Borel character [16]. This has led some authors to doubt the use of such expansions around the *lower critical dimension* altogether [17]. This would be quite unfortunate, since it would jeopardize other interesting theories such as Anderson's theory of localization [18]. The basis of these doubts is the increasing relevance of higher powers of the derivative term [19]. However, hope for the utility of these expansions is not completely lost, since the argument requires interchanging two limits: one is the analytic continuation in ϵ, the other is the increasing to infinity of the number of derivatives [20]. The purpose of this section is to sustain this hope by combining the expansions in $2+\epsilon$ diemnsions with the previous expansions in $4-\varepsilon$ dimensions to obtain precise critical exponents for all dimensions D between four and two. This will be done explicitly [21] only for the critical exponent ν and the universality classes $N = 3, 4, 5$.

So far, the ϵ-expansions of ν^{-1} and the anomalous dimension η have been calculated up to the powers ϵ^4 [22]:

$$\nu^{-1} = \epsilon + \frac{\epsilon^2}{N-2} + \frac{\epsilon^3}{2(N-2)} - \left[30-14N+N^2+(54-18N)\zeta(3)\right]\frac{\epsilon^4}{4(N-2)^3} + \dots \ . \quad (19.111)$$

$$\eta = \frac{\epsilon}{N-2} - \frac{(N-1)\,\epsilon^2}{(N-2)^2} + \frac{N\,(N-1)\,\epsilon^3}{2\,(N-2)^3} - (N-1)\left[-6+2\,N+N^2+(-12+N+N^2)\,\zeta(3)\right]\frac{\epsilon^4}{4\,(N-2)^4} + \dots \ . \quad (19.112)$$

When evaluated at $\epsilon = 1$, the first series yields for the three-dimensional O(3)-model the diverging successive values $\nu^{-1} = (1,\ 2,\ 2.5\,,3.25)$. Padé approximations do not help; the best of them, the [1,2]-approximation, gives the too large value $\nu = 2$. So far, the only result which is not far from the true value has been obtained via the Padé-Borel transform

$$P^{[1,2]}(\epsilon, t) = \frac{\epsilon t}{1 - \epsilon t/2 + \epsilon^2 t^2/6}, \quad (19.113)$$

from which we obtain the ϵ-dependent critical exponent

$$\nu^{-1}(\epsilon) = \int_0^\infty dt\, e^{-t} P^{[1,2]}(\epsilon, t), \quad (19.114)$$

whose value at $\epsilon = 1$ is ≈ 1.252, corresponding to $\nu \approx 0.799$ still too large to be useful. The other Padé-Borel approximants are singular and thus of no use, as shown in Fig. 19.17.

The full ϵ-dependence of the power series (19.111) and the Padé-Borel-approximation (19.114) can be seen in Fig. 19.18 on page 360.

A direct evaluation of the series for the anomalous dimension η yields the even worse values $(2,\ -2,\ 4,\ -5)$. Here the nonsingular Borel-Padé approximations $[2,1]$, $[1,2]$, and $[1,1]$ yield 0.147, 0.150, and 0.139, rather than the correct value 0.032. The full ϵ-dependence of the power series (19.112) and the Padé[2,1]-Borel-approximation are also shown in Fig. 19.18.

The remedy for these problems comes from the strong-coupling theory of Section 19.2. It allows us to find an extended variational perturbation expansion if we know not only L weak-coupling coefficients but also M strong-coupling expansion coefficients. We merely add to the set of coefficients $f_1, \dots, f_L$ a set of M unknown ones, $f_{L+1}, \dots, f_{L+M}$, and determine the latter via a fit of the resulting strong-coupling coefficients $b_0, \dots, b_{M-1}$ of Eq. (19.14) to the known ones.

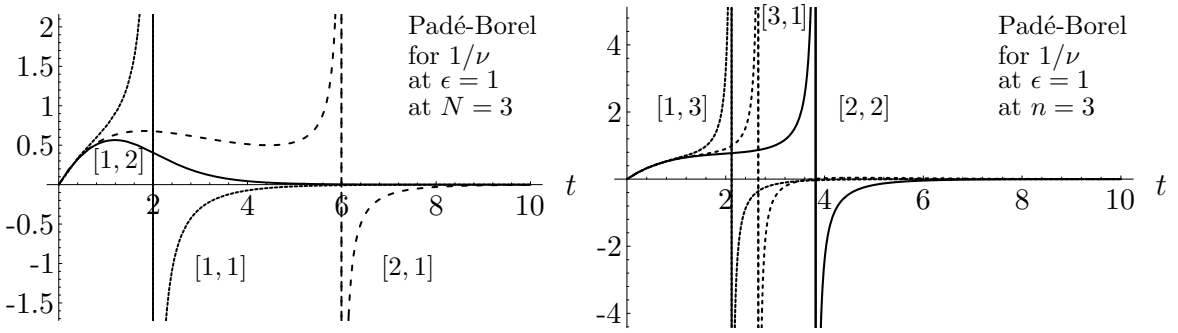

FIGURE 19.17 Integrands of the Padé-Borel transform (19.114) for the Padé approximants [1,1], [2,1], [1,2] and for [1,3], [3,1], [2,2] at $\epsilon = 1$. Only the last is integrable, yielding $\nu^{-1} \approx 1.25183 \approx 1/.79883$.

19.8.1 Critical Exponent ν.

This procedure will now be applied to the perturbation expansion (19.111) for ν^{-1} in $2+\epsilon$ dimensions, considering it as the *strong-coupling expansion* of a series in the variable $\tilde{\varepsilon} = 2(4-D)/(D-2) = 4(1-\epsilon/2)/\epsilon = \varepsilon/(1-\varepsilon/2)$:

$$\begin{aligned}\nu^{-1} &= 4\,\tilde{\varepsilon}^{-1} - 8\frac{N-4}{N-2}\,\tilde{\varepsilon}^{-2} + 16\frac{N-4}{N-2}\,\tilde{\varepsilon}^{-3} \\ &\quad - 32\left[52 - 16N - 4N^2 + N^3 + 36\,(3-N)\,\zeta(3)\right]\frac{\tilde{\varepsilon}^{-4}}{(N-2)^3} + \dots\ .\end{aligned} \tag{19.115}$$

The weak-coupling expansion of this series is obtained from Eq. (17.14) by a change of variables from ε to $\tilde{\varepsilon}$, and a re-expansion:

$$\begin{aligned}\nu^{-1} = 2 &- \frac{N+2}{N+8}\tilde{\varepsilon} + \left(20+3\,N+N^2\right)\frac{(2+N)\tilde{\varepsilon}^2}{2\,(8+N)^3} + \left[-2240-624\,N-212\,N^2-9\,N^3-2\,N^4+8\cdot 12(8+N)(22+5\,N)\zeta(3)\right]\frac{(2+N)\tilde{\varepsilon}^3}{8\,(8+N)^5} \\ &+ \Big[5\left(568576+382144\,N+103920\,N^2+9532\,N^3+1142\,N^4+21\,N^5+4\,N^6\right) \\ &+80\left(-249600-148960\,N-42912\,N^2-6516\,N^3-350\,N^4+3\,N^5\right)\zeta(3)+80\cdot 18\,(8+N)^3\,(22+5N)\,\zeta(4) \\ &-80\cdot 80\,(8+N)^2\left(186+55N+2N^2\right)\zeta(5)\Big]\frac{(2+N)}{160\,(8+N)^7}\tilde{\varepsilon}^4 \\ &+ \Big[945\left(-105091072-106771456\,N-47635968\,N^2-11768576\,N^3-1835504\,N^4-122812\,N^5-6270\,N^6-45\,N^7-8\,N^8\right) \\ &+15120\left(57911296+46323968\,N+17913728\,N^2+3869024\,N^3+514592\,N^4+46900\,N^5+1902\,N^6-37\,N^7\right)\zeta(3) \\ &+15120\left(-47874048-40615936\,N-11928064\,N^2-1525888\,N^3-89408\,N^4-3200\,N^5-128\,N^6\right)\zeta^2(3) \\ &+945\left(101376+61056\,N+13392\,N^2+1278\,N^3+45\,N^4\right)\zeta(4) \\ &+256\cdot 945\,(8+N)^2\left(345552+193822\,N+48749\,N^2+6506\,N^3+235\,N^4\right)\zeta(5) \\ &+945\cdot 56448\,(8+N)^3\left(526+189\,N+14\,N^2\right)\zeta(7)\Big]\frac{(N+2)\tilde{\varepsilon}^5}{120960\,(8+N)^9} + \dots\ ,\end{aligned}$$

whose numerical forms are for $N = 3, 4, 5$

$$N=3:\ \nu^{-1} = 2 - 0.45455\,\tilde{\varepsilon} + 0.071375\,\tilde{\varepsilon}^2 + 0.15733\,\tilde{\varepsilon}^3 - 0.52631\,\tilde{\varepsilon}^4 + 1.5993\,\tilde{\varepsilon}^5 \tag{19.116}$$

$$N=4:\ \nu^{-1} = 2 - 0.5\,\tilde{\varepsilon} + 0.0833333\,\tilde{\varepsilon}^2 + 0.147522\,\tilde{\varepsilon}^3 - 0.499944\,\tilde{\varepsilon}^4 + 1.47036\,\tilde{\varepsilon}^5, \tag{19.117}$$

$$N=5:\ \nu^{-1} = 2 - 0.538462\,\tilde{\varepsilon} + 0.0955849\,\tilde{\varepsilon}^2 + 0.135442\,\tilde{\varepsilon}^3 - 0.469842\,\tilde{\varepsilon}^4 + 1.34491\,\tilde{\varepsilon}^5, \tag{19.118}$$

$$N=1:\ \nu^{-1} = 2 - 0.333333\,\tilde{\varepsilon} + 0.0493827\,\tilde{\varepsilon}^2 + 0.158478\,\tilde{\varepsilon}^3 - 0.539937\,\tilde{\varepsilon}^4 + 1.78954\,\tilde{\varepsilon}^5. \tag{19.119}$$

Extending these series by four more terms $f_6\,\tilde{\varepsilon}^6 + f_7\,\tilde{\varepsilon}^7 + f_8\,\tilde{\varepsilon}^8 + f_9\,\tilde{\varepsilon}^9$, we calculate the functions $b_n(\hat{g}_B)$ of Eq. (19.11), and from these the strong-coupling coefficients $\bar{b}_0, \bar{b}_1, \bar{b}_2, \bar{b}_3$, in (19.14) as

described there, [after having identified g_B with $\tilde{\varepsilon}$, and the parameters (p, q) with $(-2, 2)$]. The coefficients $f_6\,, f_7,\ f_8,\ f_9$ are determined to make (19.14) agree with the expansion coefficient (19.115) [23]. The results are shown in Tables 19.5 –19.8 .

TABLE 19.5 Coefficients of successive extensions of expansion coefficients in Eq. (19.116) of ν^{-1} with $N = 3$ determined from the strong-coupling coefficients (4, 8, −16, 160) of Eq. (19.115) for $M = 1, 2, 3, 4$.

M	f_6	f_7	f_8	f_9
1	−203.827			
2	−5.67653	17.6165		
3	−4.25622	9.04109	−15.7331	
4	−3.80331	6.87304	−10.0012	12.3552

TABLE 19.6 Same as above for the expansion coefficients in Eq. (19.117) of ν^{-1} with $N = 4$. They are determined from the strong-coupling coefficients (4, 0, 0, 221.096) of Eq. (19.115) for $M = 1, 2, 3, 4$.

M	f_6	f_7	f_8	f_9
1	−147.508			
2	−7.91064	37.1745		
3	−4.59388	12.3044	−27.0837	
4	−3.72613	7.47851	−12.2129	16.9547

TABLE 19.7 Same as above the expansion coefficients in Eq. (19.118) of ν^{-1} with $N = 5$. They are determined from the strong-coupling coefficients (8, −8/3, 16/3, 106.131) of Eq. (19.115) for $M = 1, 2, 3, 4$.

M	f_6	f_7	f_8	f_9
1	−108.648			
2	−10.1408	60.7217		
3	−4.75598	15.1045	−38.9689	
4	−3.57909	7.84272	−14.1142	21.6045

TABLE 19.8 Coefficients of successive extensions of expansion coefficients in Eq. (19.119) of ν^{-1} with $N = 1$, determined from $M = 1, 2, 3, 4$ strong-coupling coefficients (4, −24, 48, 3825.54) of Eq. (19.115).

M	f_6	f_7	f_8	f_9
1	−413.921			
2	−5.25285	12.1104		
3	−442759	12450066	−196950675	
4	−5.7343	13.7134	−25.226	38.0976

In order to see how the result improves with the number M of additional strong-coupling coefficients, we go through this procedure successively for $M = 1, 2, 3, 4$. The four resulting curves for $\nu^{-1}(\varepsilon)$ of the O(N) universality classes with $N = 3, 4, 5$ are shown in Figs. 19.18–19.20. In each figure, we have also plotted successive critical exponents ν at $\varepsilon = 1$ as a function of the variable $x = M^{-2}$, which makes them lie approximately on a straight line intercepting the ν-axis at the limiting value ν_∞. This extrapolated value is in excellent agreement with the seven-loop determination of critical exponents to be described in the next chapter. See in particular Table 20.2 .

Finally, we plot our highest ($M = 4$) approximations for $N = 3, 4, 5$ together with the large-N approximations for $N = \infty, 20, 10, 6$ in Fig. 19.21 to see the trend for increasing N, which shows that the latter for $N = 6$ is still far from the exact curve [24].

The relation between the ϵ- and ε-expansions is expected to be restricted to $N > 2$ for physical reasons. It is instructive to see that the variational interpolation method reflects this problem in two places. First, the expansion coefficients in Table 19.8 show a large irregularity for $N = 1$. Second, the successive approximations for ν^{-1} in Fig. 19.22 display no tendency of convergence with increasing order M of approximation.

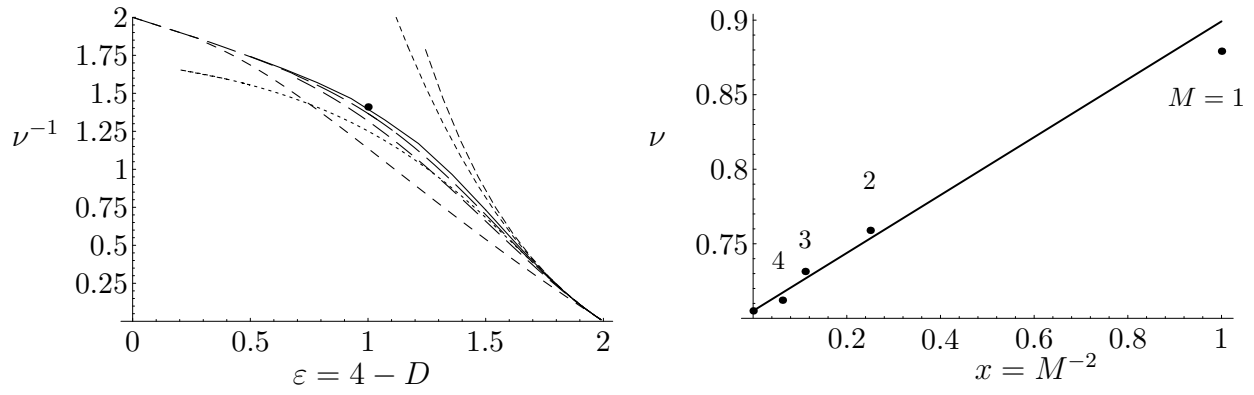

FIGURE 19.18 Inverse of critical exponent ν for classical Heisenberg model in O(3)-universality class, plotted as a function of $\varepsilon = 4-D$. Solid curve is obtained from variational interpolation between five-loop ε-expansion of ϕ^4-theory near $D = 4$ dimensions, and four-loop ϵ-expansion (19.111) of nonlinear σ-model around $D = 2$ dimensions. Long-dashed curves are successive approximations using strong-coupling expansion (19.115) up to the first, second, and third order. Short-dashed curves display the first three and four terms of ϵ-expansion and the associated Padé [1,2]-Borel approximations (lowest curve). The dot shows seven-loop results in $D = 3$ dimensions, $\nu = 0.705$. Values from our successive interpolations are $(\nu_1, \nu_2, \nu_3, \nu_4) = (0.87917, 0.75899, 0.731431, 0.712152)$. On the right, these values are extrapolated to infinite order by plotting them against $x = M^{-2}$ which makes them lie on a straight line with the intercept $\nu_\infty = 0.705$, in excellent agreement with the seven-loop result.

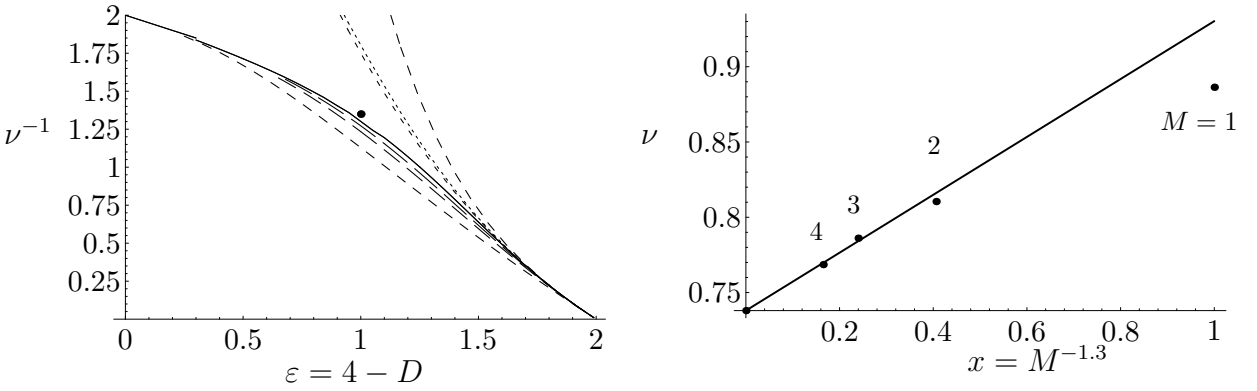

FIGURE 19.19 Analog of Fig. 19.18 ν^{-1} in for O(4)-universality class. The dot shows the six-loop result in $D = 3$ dimensions, $\nu = 0.737$. Values from our successive interpolation are $(\nu_1, \nu_2, \nu_3, \nu_4) = (0.88635, 0.810441, 0.786099, 0.768565)$. On the right, these values are extrapolated to infinite order by plotting them against $x = M^{-1.3}$, which makes them lie roughly on a straight line with intercept $\nu_\infty = 0.738$, in reasonable agreement with the six-loop result $\nu = 0.737$ (slightly worse than for $N = 3$, 4).

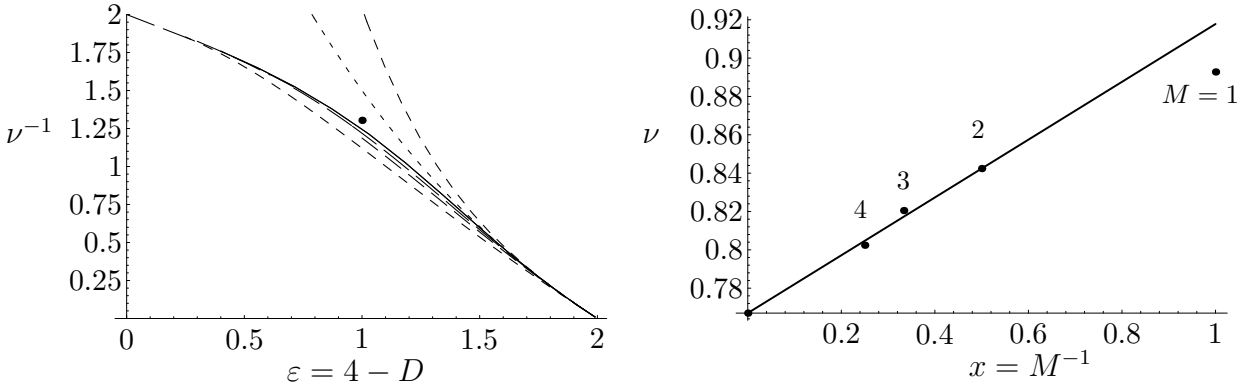

FIGURE 19.20 Analog of previous two figures for ν^{-1} in O(5)-universality class. Values from our successive interpolation are $(\nu_1, \nu_2, \nu_3, \nu_4) = (0.89278, 0.842391, 0.820491, 0.802416)$. On the right, these values are extrapolated to infinite order by plotting them against $x = M^{-1}$, which makes them lie roughly on a straight line with intercept $\nu_\infty = 0.767$, in excellent agreement with the six-loop result $\nu = 0.737$.

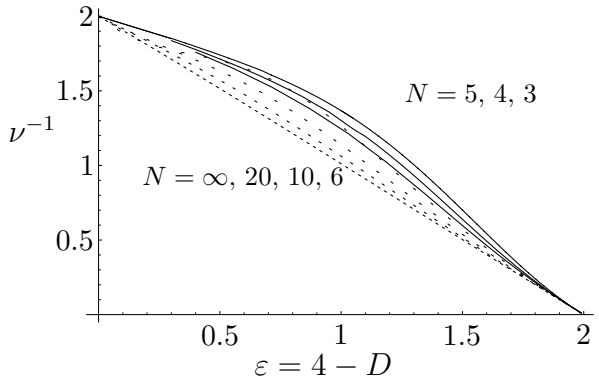

FIGURE 19.21 Highest approximations ($M = 4$) for ν^{-1} in O(N) universality class with $N = 3, 4, 5$ (counting from the top), and the $1/N$-expansions to order $1/N^2$ for $N = \infty, 20, 10, 6$ (counting from the bottom). The sixth-order result is still far from the exact one.

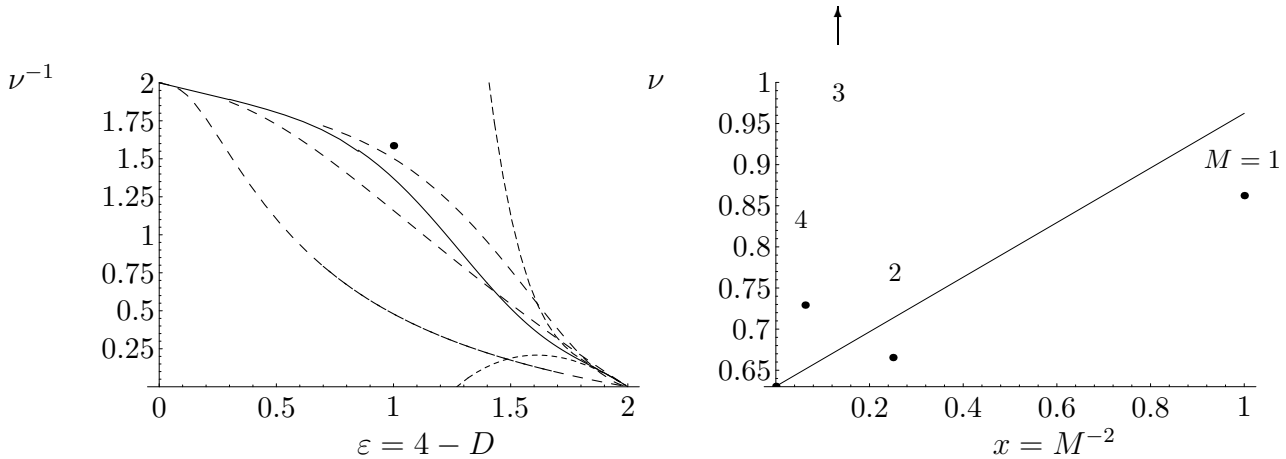

FIGURE 19.22 Same plot as in Fig. 19.18, but for ν^{-1} in O(1)-universality class (of Ising model). Again there is no Padé-Borel approximation. The dot represents seven-loop result in $D = 3$ dimensions $\nu = 0.6305$. The four interpolations give $(\nu_1, \nu_2, \nu_3, \nu_4) = (0.862357, 0.665451, 2.08686, 0.729231)$. They show no tendency of convergence towards the seven-loop exponent.

19.8.2 Critical Exponent η.

For the critical exponent η, the series (19.112) reads in the variable $\tilde{\varepsilon}$:

$$\eta = 4\frac{\tilde{\varepsilon}^{-1}}{N-2} + 8(4-3N)\frac{\tilde{\varepsilon}^{-2}}{(N-2)^2} + 16(12-18N+7N^2)\frac{\tilde{\varepsilon}^{-3}}{(N-2)^3}$$
$$+ 32\left[\left(20-56N+52N^2-15N^3\right)+2(N-1)\left(12-N-N^2\right)\zeta(3)\right]\frac{\tilde{\varepsilon}^{-4}}{(N-2)^4} + \dots, \quad (19.120)$$

whereas the weak-coupling expansion is [25]

$$\frac{\eta}{\epsilon^2} = \frac{2+N}{2(N+8)^2} + \left(272+56\,N-N^2\right)\frac{(2+N)\,\epsilon}{8(N+8)^4} \quad (19.121)$$
$$+\left\{46144+17920\,N+1124\,N^2-230\,N^3-5\,N^4-32\cdot 12\,(22+5\,N)\,\zeta(3)\right\}\frac{(2+N)\,\epsilon^2}{32(N+8)^6}$$
$$+\Big\{5655552+2912768\,N+262528\,N^2-121472\,N^3-27620\,N^4-946\,N^5-13\,N^6$$
$$+16(N+8)\left(-171264-68672\,N-1136\,N^2+1220\,N^3+10\,N^4+N^5\right)\zeta(3)$$
$$+128\cdot 9\,(N+8)^3\,(22+5N)\,\zeta(4)+28\cdot 40\,(N+8)^2\left(186+55\,N+2\,N^2\right)\,\zeta(5)\Big\}\frac{(2+N)\,\epsilon^3}{128(N+8)^8}+\dots\,.$$

whose numerical forms are, for $N = 3, 4, 5$:

$$N=3: \quad \eta/\epsilon^2 = 5/242 + 0.0183987\,\tilde{\epsilon} - 0.0166488\,\tilde{\epsilon}^2 + 0.032432\,\tilde{\epsilon}^3 + \dots, \quad (19.122)$$
$$N=4: \quad \eta/\epsilon^2 = 1/48 + 0.0173611\,\tilde{\epsilon} - 0.0157657\,\tilde{\epsilon}^2 + 0.029057\,\tilde{\epsilon}^3 + \dots, \quad (19.123)$$
$$N=5: \quad \eta/\epsilon^2 = 7/338 + 0.0161453\,\tilde{\epsilon} - 0.0148734\,\tilde{\epsilon}^2 + 0.0259628\,\tilde{\epsilon}^3 + \dots, \quad (19.124)$$
$$N=1: \quad \eta/\epsilon^2 = 1/54 + 0.01869\,\tilde{\epsilon} - 0.0176738\,\tilde{\epsilon}^2 + 0.0386577\,\tilde{\epsilon}^3 + \dots. \quad (19.125)$$

These series can again be extended by four more terms $f_4\,\tilde{\varepsilon}^4 + f_5\,\tilde{\varepsilon}^5 + f_6\,\tilde{\varepsilon}^6 + f_7\,\tilde{\varepsilon}^7$, that make the strong-coupling coefficients $\bar{b}_0, \bar{b}_1, \bar{b}_2, \bar{b}_3$, in (19.14) agree with those in Eq. (19.120), we obtain the additional weak-coupling coefficients $f_4\,, f_5,\ f_6\,f_7$ as described above. However, here we encounter problems: the η-values from the interpolation come out too large by about a factor 2. Also γ does not interpolate well. The reason for this failure seems to be that the strong-coupling expansions (19.115) and (19.120) are divergent, whereas the interpolation yields in general *convergent* strong-coupling expansions.

Notes and References

A simple exposition of variational perturbation theory in the context of quantum mechanics can be found in the textbook in Ref. [2], which also contains citations to the numerous publications preparing the grounds for the recent progress. A certainly incomplete list is given below.
There were two main predecessors coming from different directions. From the mathematical side, the seminal paper was Ref. [3]. From the physical side, the development was triggered by Feynman and Kleinert in Ref. [1], and its systematic extension to arbitrary order in

H. Kleinert, Phys. Lett. A **173**, 332 (1993) (quant-ph/9511020).

The main steps of variation perturbation theory from quantum mechanics to quantum field theory was made in Refs. [5,6,10]. First, still in quantum mechanics, by exploiting previously

unused even approximants which do not have an extremum, as explained in Chapter 5 of the above textbook. Second, the determination of the exponent ω of approach to scaling from the assumption of scaling behavior in the strong-coupling limit, and third, a reliable extrapolation procedure to infinite order on the basis of the theoretically known analytic order dependence (the latter being inspired by the pioneering work of Seznec and Zinn-Justin in Ref. [3]). These three improvements were essential in obtaining extremely accurate critical exponents rivaling the powerful combination of renormalization group and Borel-type resummation methods.

Here is a selected list of contributions at the level of quantum mechanics:
T. Barnes and G.I. Ghandour, Phys. Rev. D **22**, 924 (1980);
B.S. Shaverdyan and A.G. Usherveridze, Phys. Lett. B **123**, 316 (1983);
P.M. Stevenson, Phys. Rev. D **30**, 1712 (1985);
D **32**, 1389 (1985);
P.M. Stevenson and R. Tarrach, Phys. Lett. B **176**, 436 (1986);
A. Okopinska, Phys. Rev. D **35**, 1835 (1987);
D **36**, 2415 (1987);
W. Namgung, P.M. Stevenson, and J.F. Reed, Z. Phys. C **45**, 47 (1989);
U. Ritschel, Phys. Lett. B **227**, 44 (1989);
Z. Phys. C **51**, 469 (1991);
M.H. Thoma, Z. Phys. C **44**, 343 (1991);
I. Stancu and P.M. Stevenson, Phys. Rev. D **42**, 2710 (1991);
R. Tarrach, Phys. Lett. B **262**, 294 (1991);
H. Haugerud and F. Ravndal, Phys. Rev. D **43**, 2736 (1991);
A.N. Sissakian, I.L. Solivtosv, and O.Y. Sheychenko, Phys. Lett. B **313**, 367 (1993);
A. Duncan and H.F. Jones, Phys. Rev. D **47**, 2560 (1993);

For the anharmonic oscillator, the highest accuracy in the strong-coupling limit was reached with exponentially fast convergence in
W. Janke and H. Kleinert, Phys. Rev. Lett. **75**, 2787 (1995) (quant-ph/9502019).
That paper contains references to earlier less accurate calculations of strong-coupling expansion coefficients from weak-coupling perturbation theory, in particular
F.M. Fernández and R. Guardiola, J. Phys. A **26**, 7169 (1993);
F.M. Fernández, Phys. Lett. A **166**, 173 (1992);
R. Guardiola, M.A. Sol´**i**s, and J. Ros, Nuovo Cimento B **107**, 713 (1992).
A.V. Turbiner and A.G. Ushveridze, J. Math. Phys. **29**, 2053 (1988);
B. Bonnier, M. Hontebeyrie, and E.H. Ticembal, J. Math. Phys. **26**, 3048 (1985);
These works were yet unable to extract the exponential law of convergence from their data.

This was shown to be related to the convergence radius of the strong-coupling expansion in Ref. [4]. Predecessors of these works which did not yet explain the exponentially fast convergence in the strong-couplings limit were
I.R.C. Buckley, A. Duncan, and H.F. Jones, Phys. Rev. D **47**, 2554 (1993);
C.M. Bender, A. Duncan, and H.F. Jones, Phys. Rev. D **49**, 4219 (1994);
A. Duncan and H.F. Jones, Phys. Rev. D **47**, 2560 (1993);
C. Arvanitis, H.F. Jones, and C.S. Parker, Phys. Rev. D **52**, 3704 (1995) (hep-th/9502386);
R. Guida, K. Konishi, and H. Suzuki, Annals Phys. **241**, 152 (1995) (hep-th/9407027).

The individual citations in the text refer to:

[1] R.P. Feynman, H. Kleinert, Phys. Rev. A **34**, 5080 (1986) (http://www.physik.fu-berlin.de/˜kleinert/159).

[2] See Chapters 5 and 17 in the textbook
H. Kleinert, *Path Integrals in Quantum Mechanics, Statistics and Polymer Physics,* World Scientific Publishing Co., Singapore 1995 (www.physik.fu-berlin.de/˜kleinert/b5).

[3] R. Seznec and J. Zinn-Justin, J. Math. Phys. **20**, 1398 (1979).

[4] H. Kleinert and W. Janke, Phys. Lett. A **206**, 283 (1995);
R. Guida K. Konishi, and H. Suzuki, Ann. Phys. **249**, 106 (1996).

[5] H. Kleinert, Phys. Lett. A **207**, 133 (1995) (quant-ph/9507005).

[6] H. Kleinert, Phys. Rev. D **57**, 2264 (1998) (www.physik.fu-berlin.de/˜kleinert/re3.html #257); addendum (cond-mat/9803268); Phys. Rev. D **60**, 85001 (1999) (hep-th/9812197).

[7] The general discussion is contained in the forthcoming 3rd edition of the textbook [2] available on the internet.

[8] W. Janke and H. Kleinert, Phys. Rev. Lett. **75**, 2787 (1995) (quant-ph/9502019).

[9] For the anharmonic oscillator where $p = 1/3$ and $q = 3$, the proof is found in Ref. [4]. The generalization to any p, q was given in Ref. [6].

[10] H. Kleinert, Phys. Lett. B **434**, 74 (1998) (cond-mat/9801167); ibid. B **463**, 69 (1999) (cond-mat/9906359).

[11] For a discussion of such contributions see
B.G. Nickel, Physica A *177*, 189 (1991);
A. Pelissetto and E. Vicari, Nucl. Phys. B *519*, 626 (1998);
522, 605 (1998); Nucl. Phys. Proc. Suppl. *73*, 775 (1999). See also the review article by these authors in cond-mat/0012164.

[12] H. Kleinert and B. Van den Bossche, (cond-mat/0011329)

[13] H. Kleinert and V. Schulte-Frohlinde, J. Phys. A **34** 1037 (2001) (cond-mat/9907214).

[14] R. Guida, J. Zinn-Justin, J. Phys. A **31**, 8130 (1998) (cond-mat/9803240).

[15] J. Kosterlitz and D. Thouless, J. Phys. C **7**, 1046 (1973).

[16] S. Hikami and E. Brézin, J. Phys. A **11**, 1141 (1978).

[17] G.E. Castilly and S. Chakravarty, Nucl. Phys. B **485**, 613 (1997) (cond-mat/9605088).

[18] P.W. Anderson, Phys. Rev. **109**, 1429 (1958).

[19] F.J. Wegner, Z. Phys. B **78**, 33 (1990).

[20] E. Brézin and S. Hikami, Phys. Rev. B **55**, R10169 (1997) (cond-mat/9612016).

[21] H. Kleinert, Phys. Lett. A **264**, 357 (2000) (hep-th/9808145).

[22] S. Hikami and E. Brézin, J. Phys. A **11**, 1141 (1978);
W. Bernreuther and F.J. Wegner, Phys. Rev. Lett. **57**, 1383 (1986);
I. Jack, D.R.T. Jones, and N. Mohammedi, Phys. Lett. B **220**, 171 (1989), Nucl. Phys. B **322**, 431 (1989);
N.A. Kivel, A.A. Stepanenko, and A.N. Vasil'ev, Nucl.Phys. B **424**, 619 (1994) (hep-th/9308073).

[23] This technique is described in detail in Ref. [5].

[24] This can also be seen in Fig. 3 of the first paper in Ref. [6].

[25] H. Kleinert, J. Neu, V. Schulte-Frohlinde, K.G. Chetyrkin, S.A. Larin, Phys. Lett. B **272**, 39 (1991) (hep-th/9503230); Erratum ibid. **319**, 545 (1993).
See also
H. Kleinert and V. Schulte-Frohlinde, Phys. Lett. B **342**, 284 (1995) (cond-mat/9503038).